INTERNATIONAL ATOMIC ENERGY AGENCY
UNITED NATIONS EDUCATIONAL, SCIENTIFIC AND CULTURAL ORGANIZATION
INTERNATIONAL CENTRE FOR THEORETICAL PHYSICS

SMR/754 - 8

WORKSHOP ON
SCIENCE AND TECHNOLOGY OF THIN FILMS

(7 - 25 March 1994)

" Processing perspective"
&
" Formation of a new form of carbon 'amorphous diamond' "
&
" A view of some wide bandgap semiconductors "

presented by:

J. CUOMO
North Carolina State University
Dept. of Materials Science and Engineering
P.O. Box 7907
NC 27895-7907 Raleigh
U.S.A.

Jerome J. Cuomo
North Carolina State University
Dept. of Materials Sci. & Eng.
Raleigh, NC 27695

- Processing Perspective
- Formation of a New form of Carbon "Amorphous Diamond"
- A View of Some Wide Bandgap Semiconductors

Processes Present and Future

Jerome J. Cuomo

IBM Research Division
T.J. Watson Research Center
P.O. Box 218
Yorktown Heights, NY 10598

IBM

General Outline

Introduction

Brief View of Where We Came From:

- Evaporation Processes
- Diode Sputter Deposition
- Magnetrons

Where We Are:

- Evaporation/Plasma/Ion Beam Assist.
- Magnetron
- Enhanced Magnetron
- Ion Beam Deposition

Where We Might Be Headed:

- Enhanced Plasma Processes
- Directed Beam
  Energetic Condensation

"The Material is The Process"

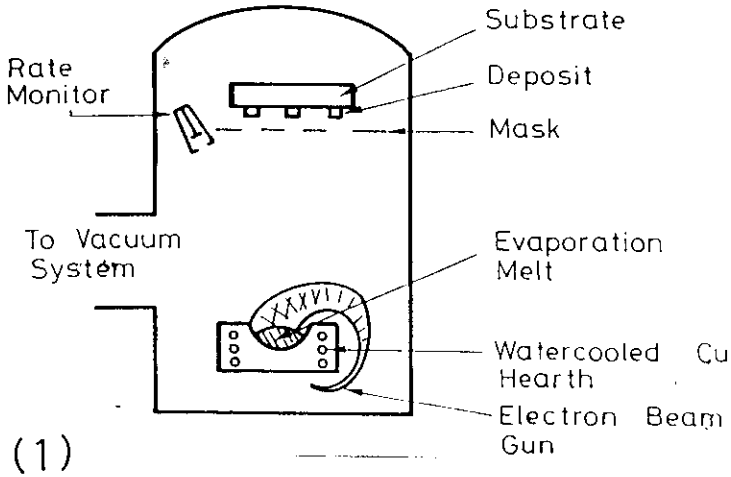

(1)

Figure 1.

Schematic of the electron beam evaporation process.

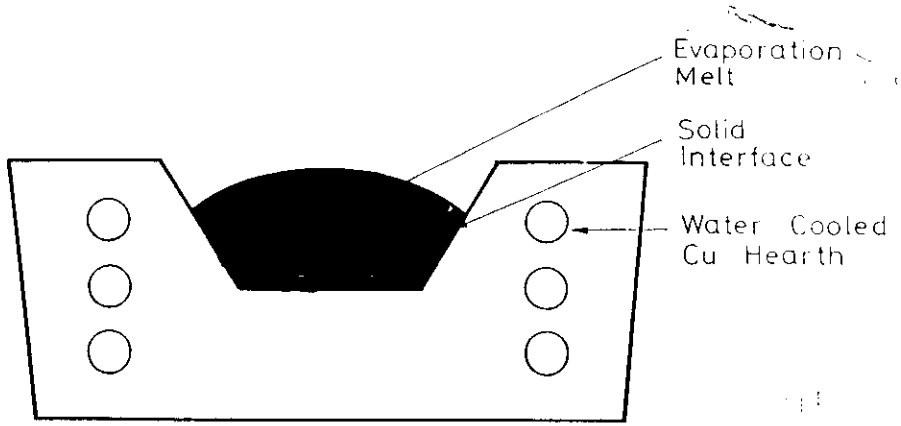

(2)

Figure 2.

Shows a water cooled copper hearth and the melt hearth interface.

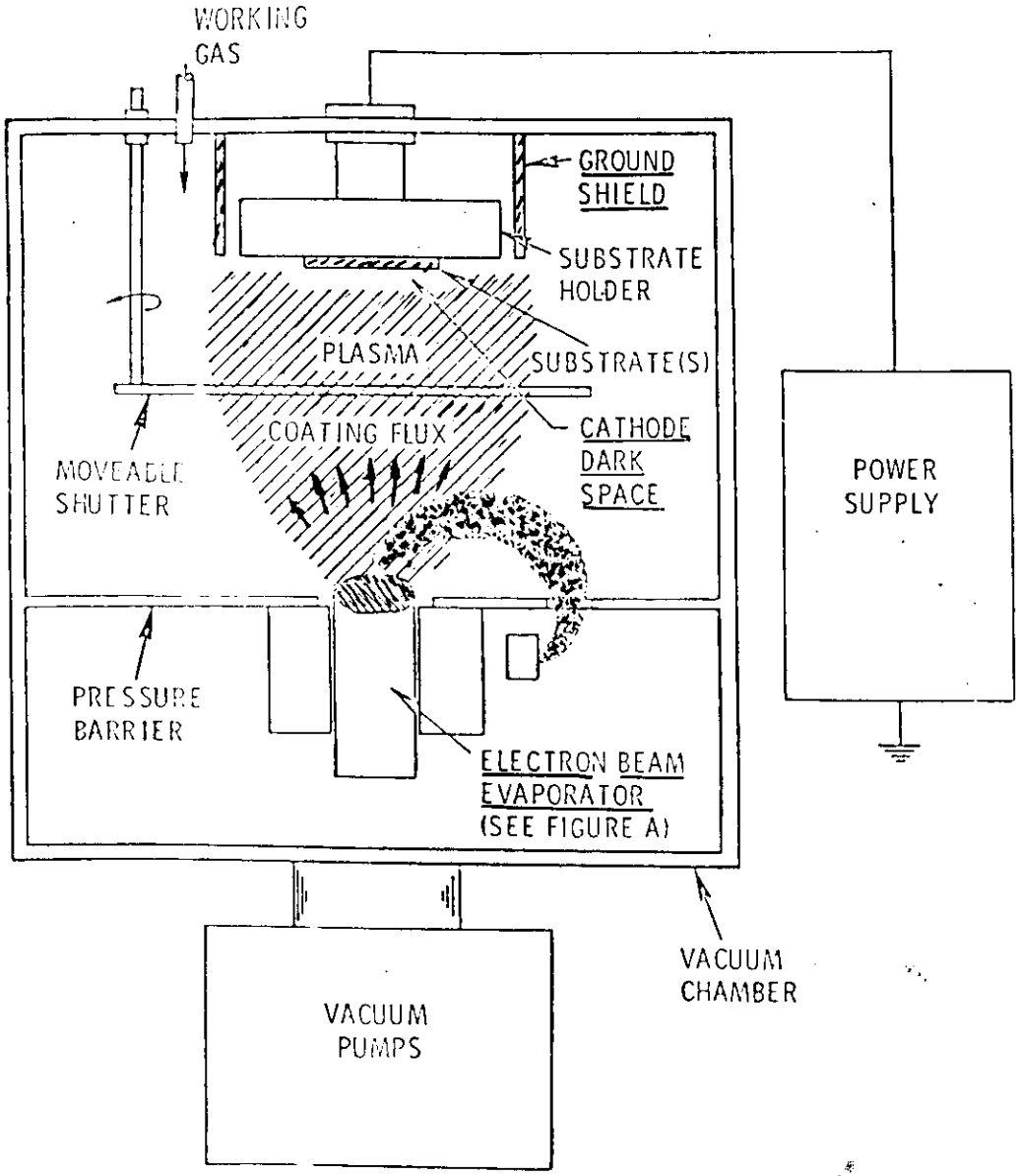

Figure 2. Ion-Plating Process.

ION PLATING

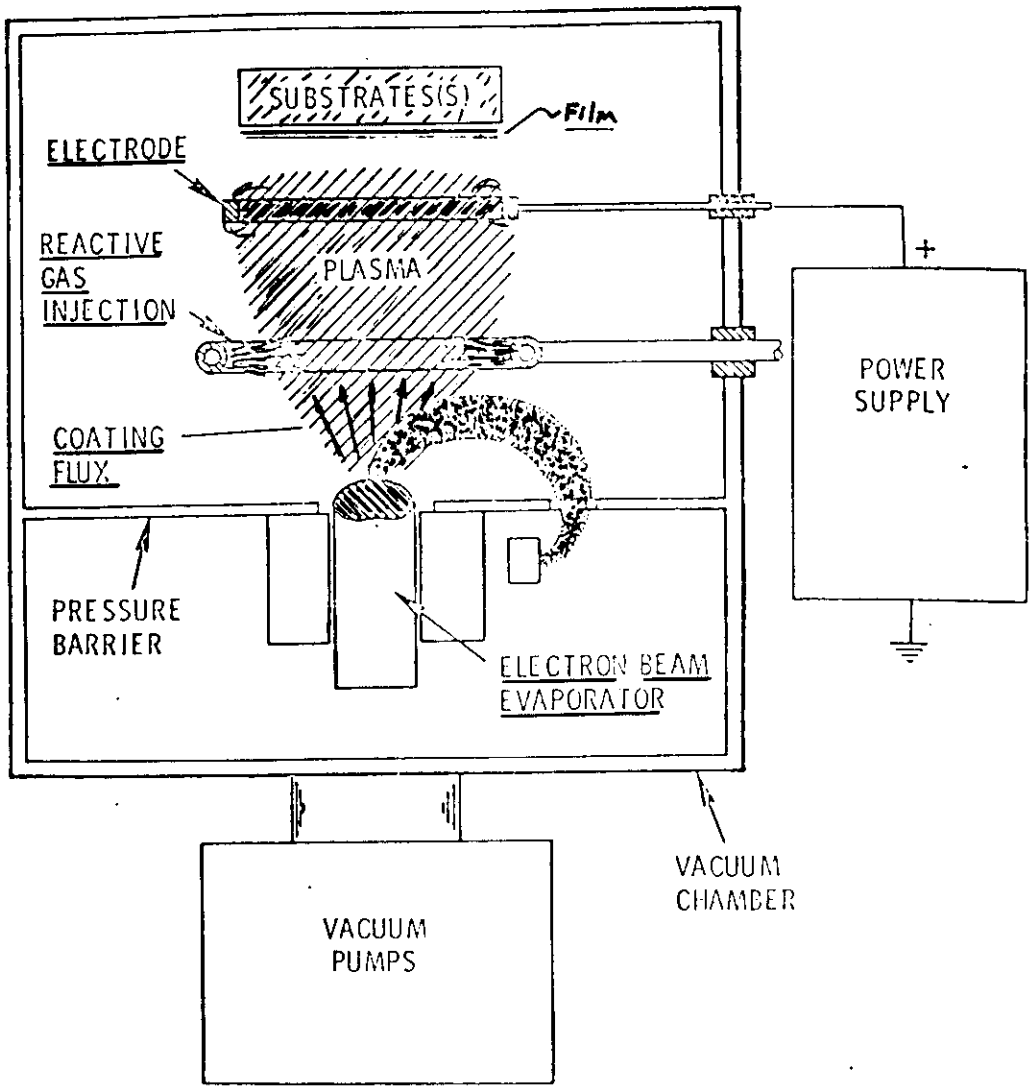

Figure 6. Schematic of the Activated Reactive Evaporation Process.

ACTIVATED REACTIVE EVAPORATION (A

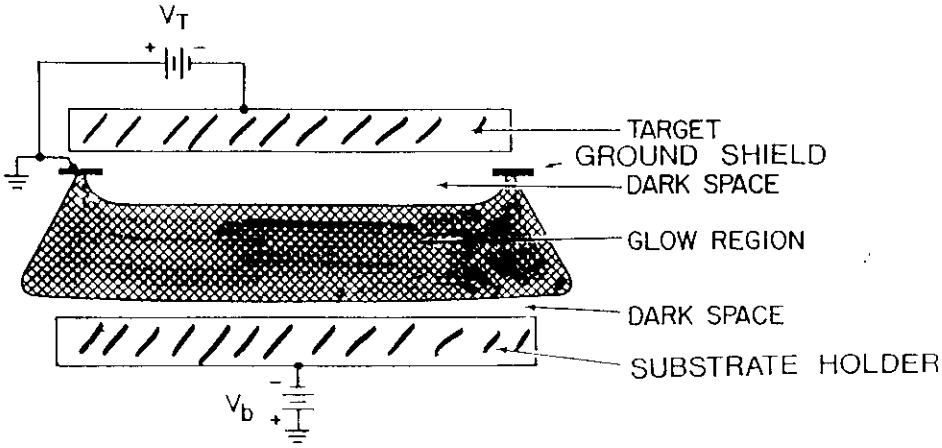

Figure 12b.

Schematic of a glow discharge as an ion source showing the target, dark space, glow region and an anode dark space when negative bias is applied to the anode.

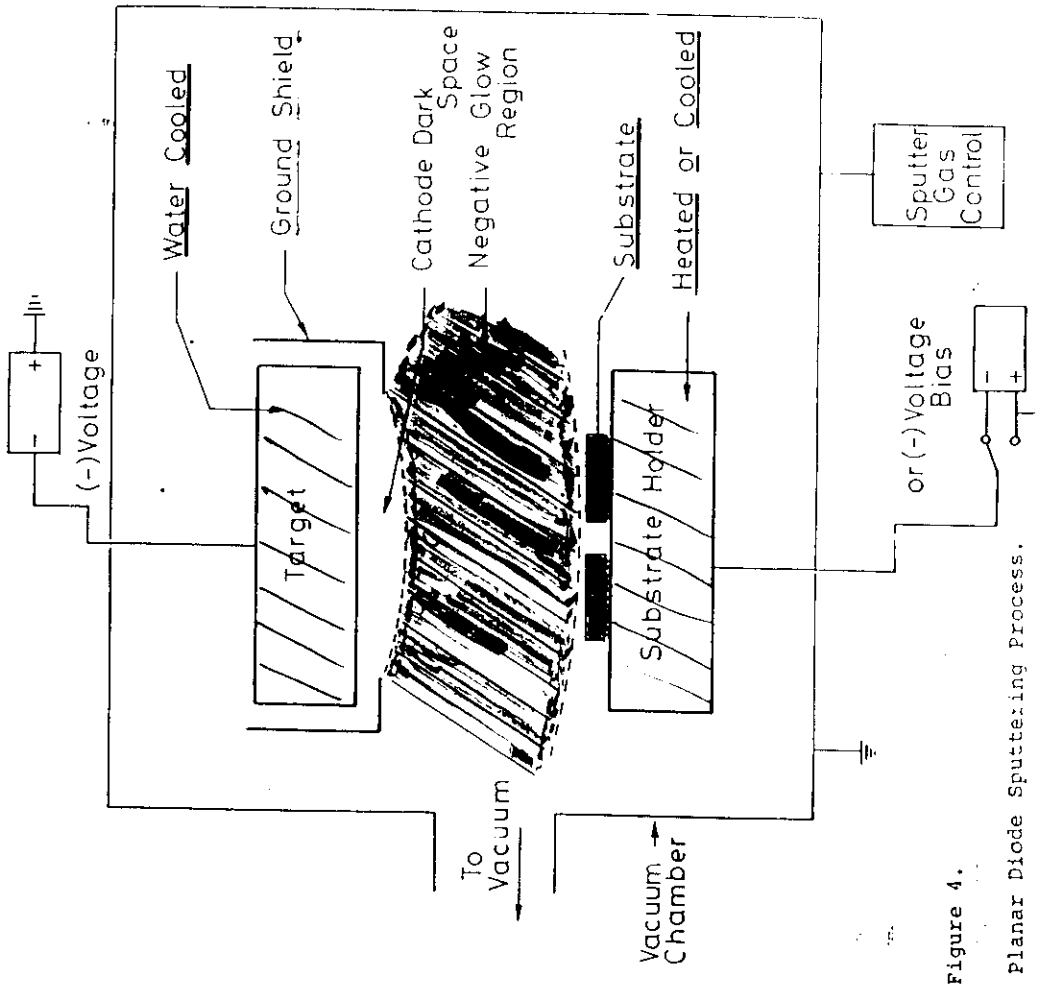

Figure 4.

tic of the Planar Diode Sputtering Process.

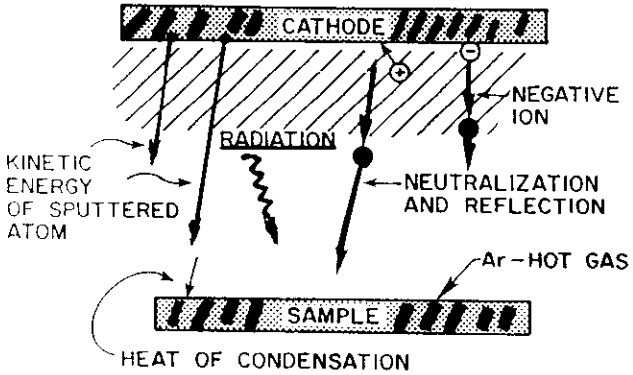

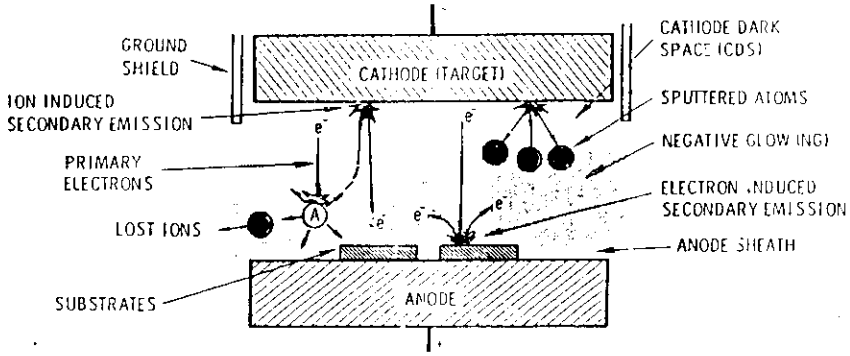

FIG. 9. Schematic representation of the plasma in a planar diode sputtering source.

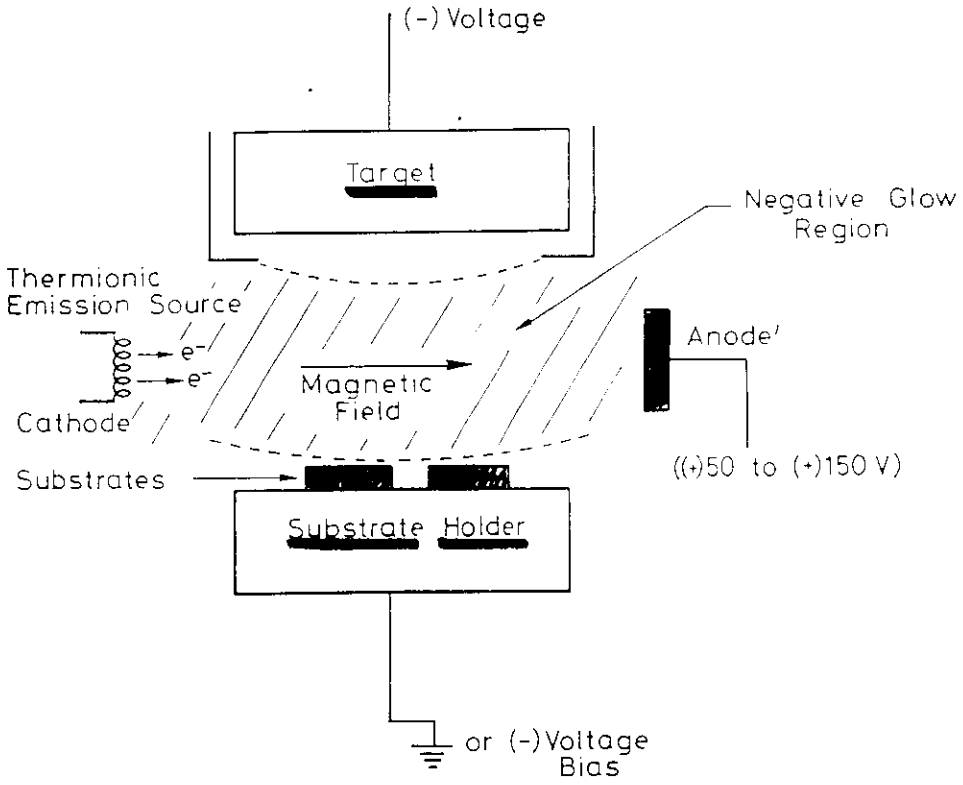

Figure 5.

Schematic of the Thermionic Assisted (triode) Sputtering Process.

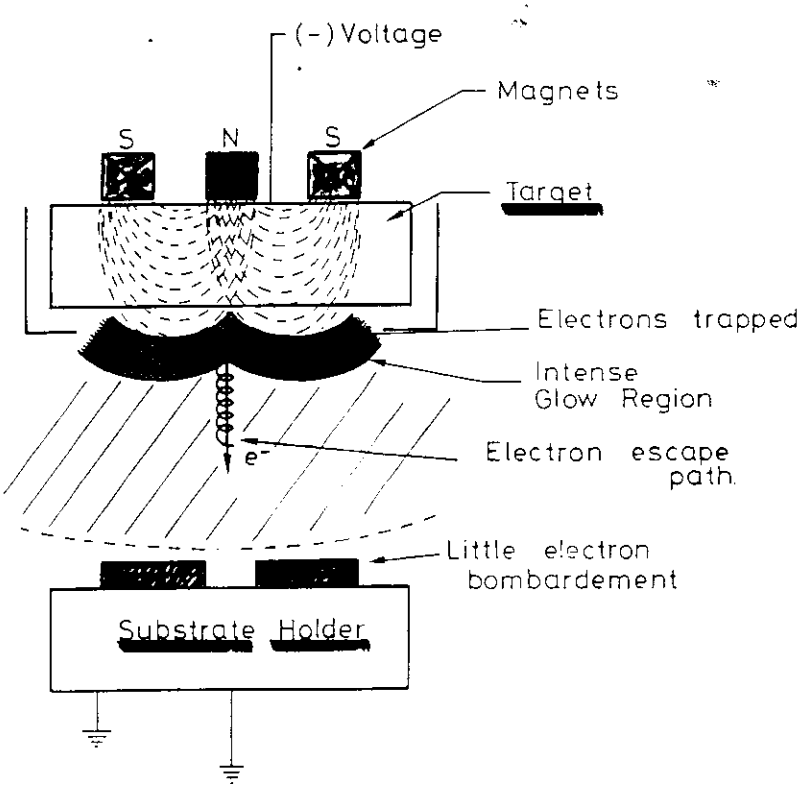

Figure 6.

Schematic of the Planar Magnetron Process.

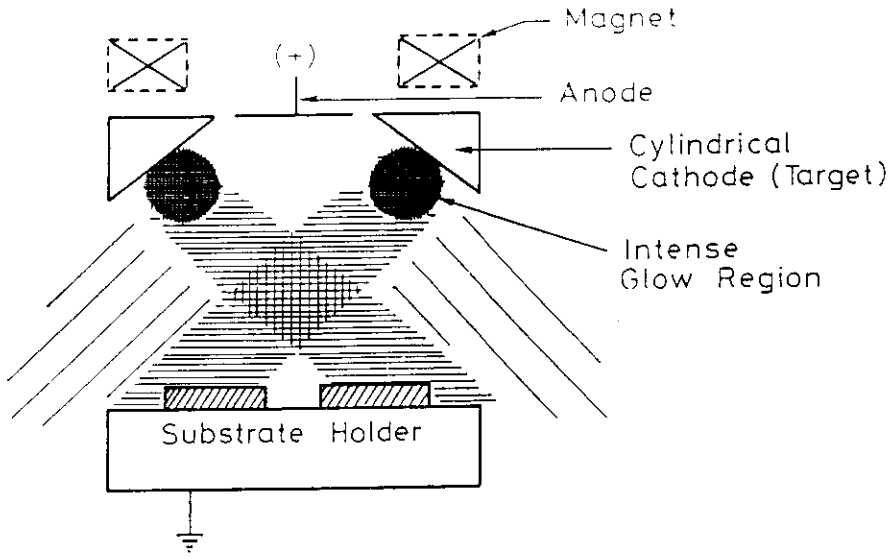

Figure 7.

Schematic of the Sputter Gun Process.

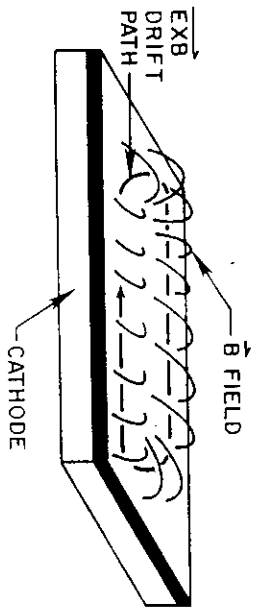

Rossnagel

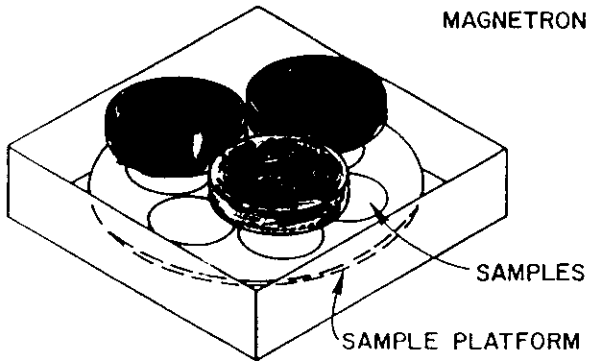

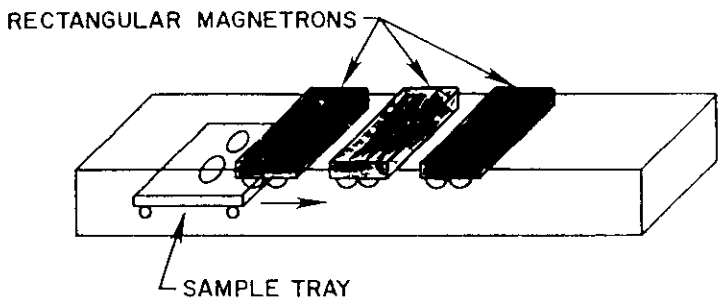

Rossnagel

Rossnagel

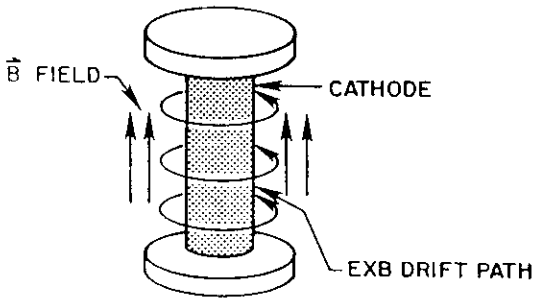
B FIELD
CATHODE
EXB DRIFT PATH

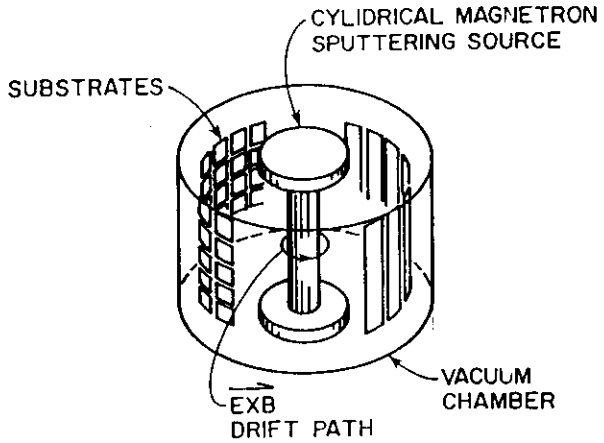
CYLIDRICAL MAGNETRON
SPUTTERING SOURCE
SUBSTRATES
VACUUM
CHAMBER
EXB
DRIFT PATH

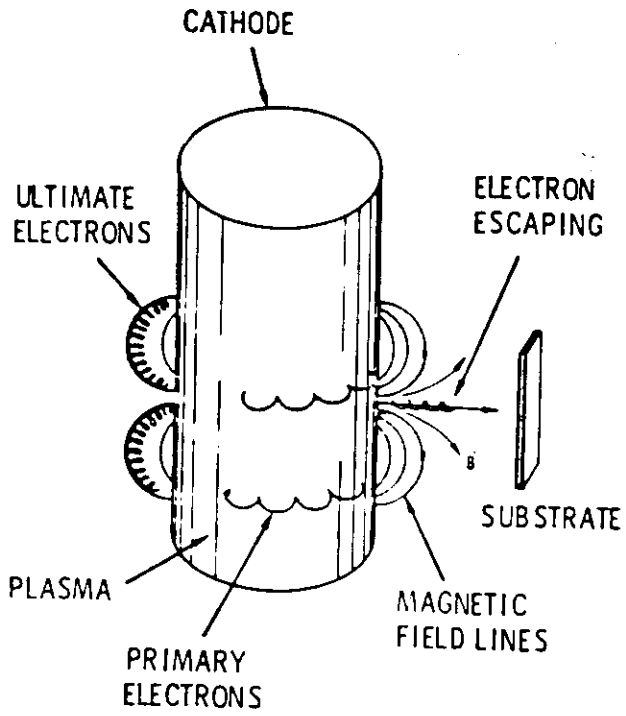

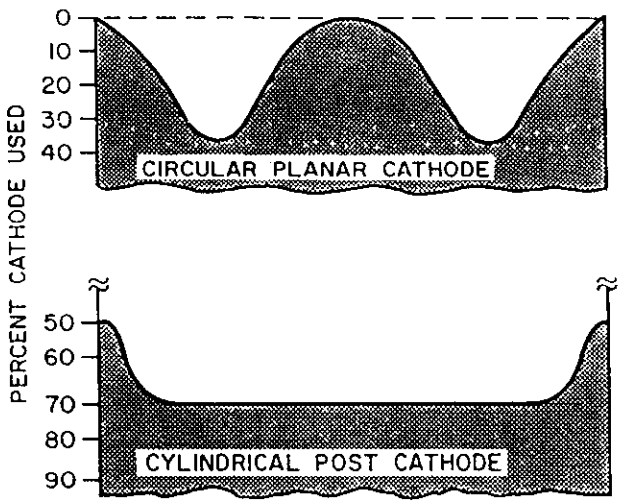

FIG. 14. Cylindrical magnetron with magnetic end confinement. From Ref. 89.

adapted from: Thornton

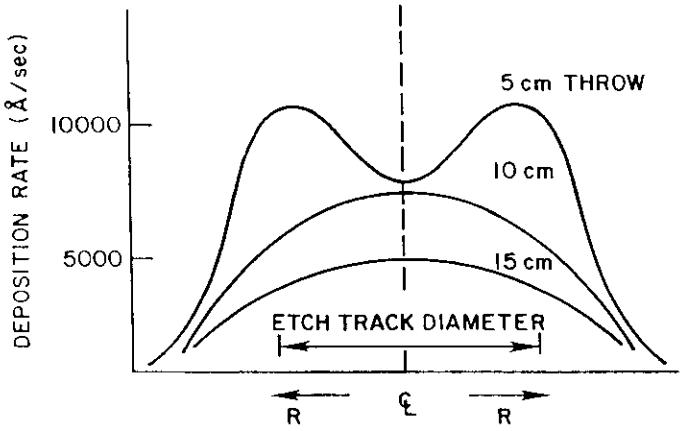
DEPOSITION RATE (Å/sec)
10000
5000
5 cm THROW
10 cm
15 cm
ETCH TRACK DIAMETER
R
℄
R

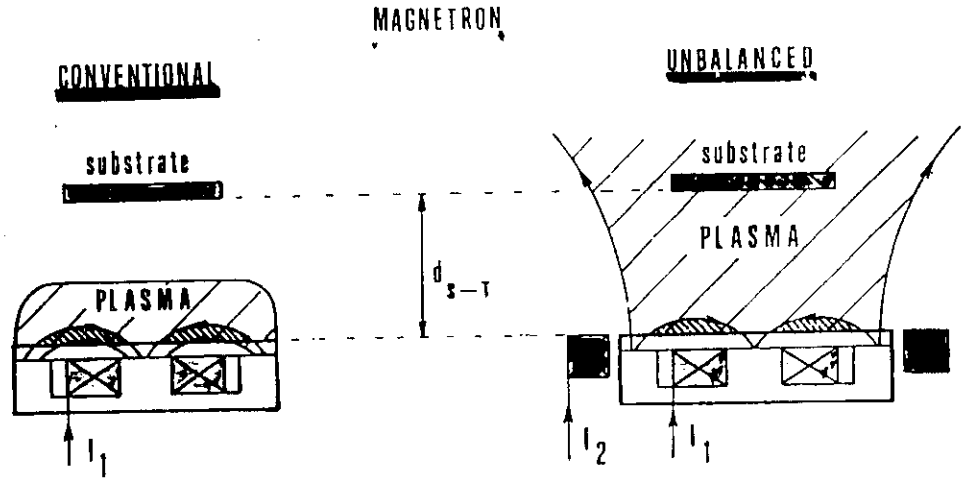
MAGNETRON
CONVENTIONAL
UNBALANCED
substrate
substrate
PLASMA
PLASMA
d_{s-T}
I_1
I_2
I_1

Hollow Cathode

Enhanced Magnetron Sputtering

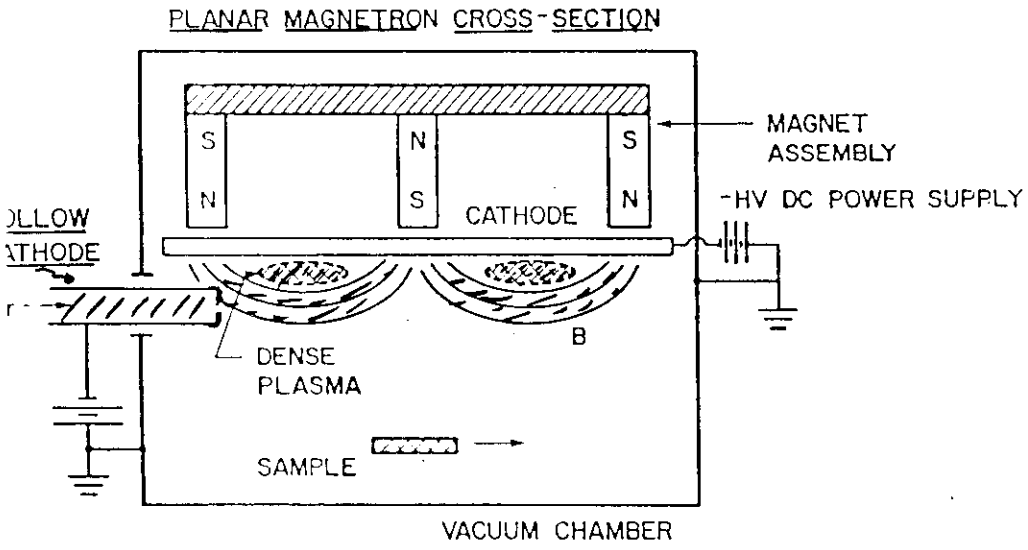

Arc Hollow Cathode Operation

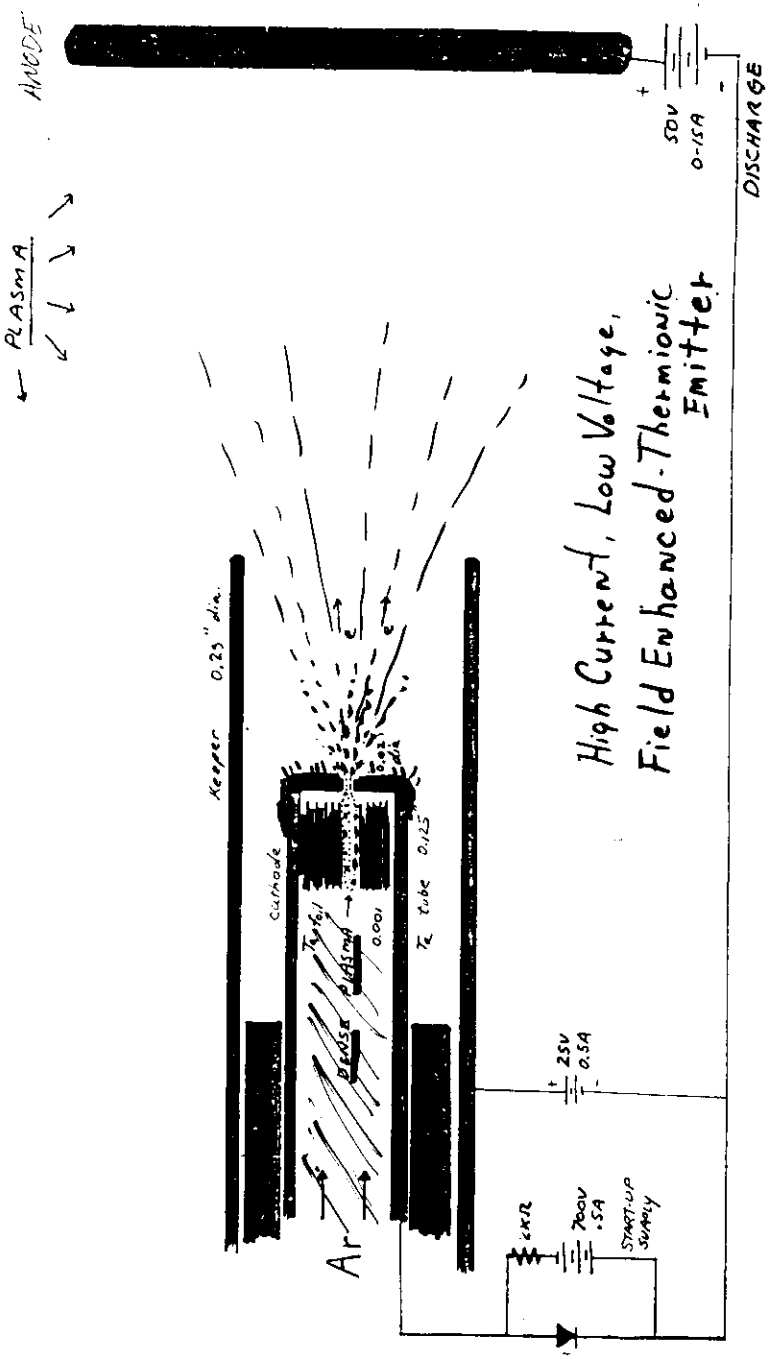

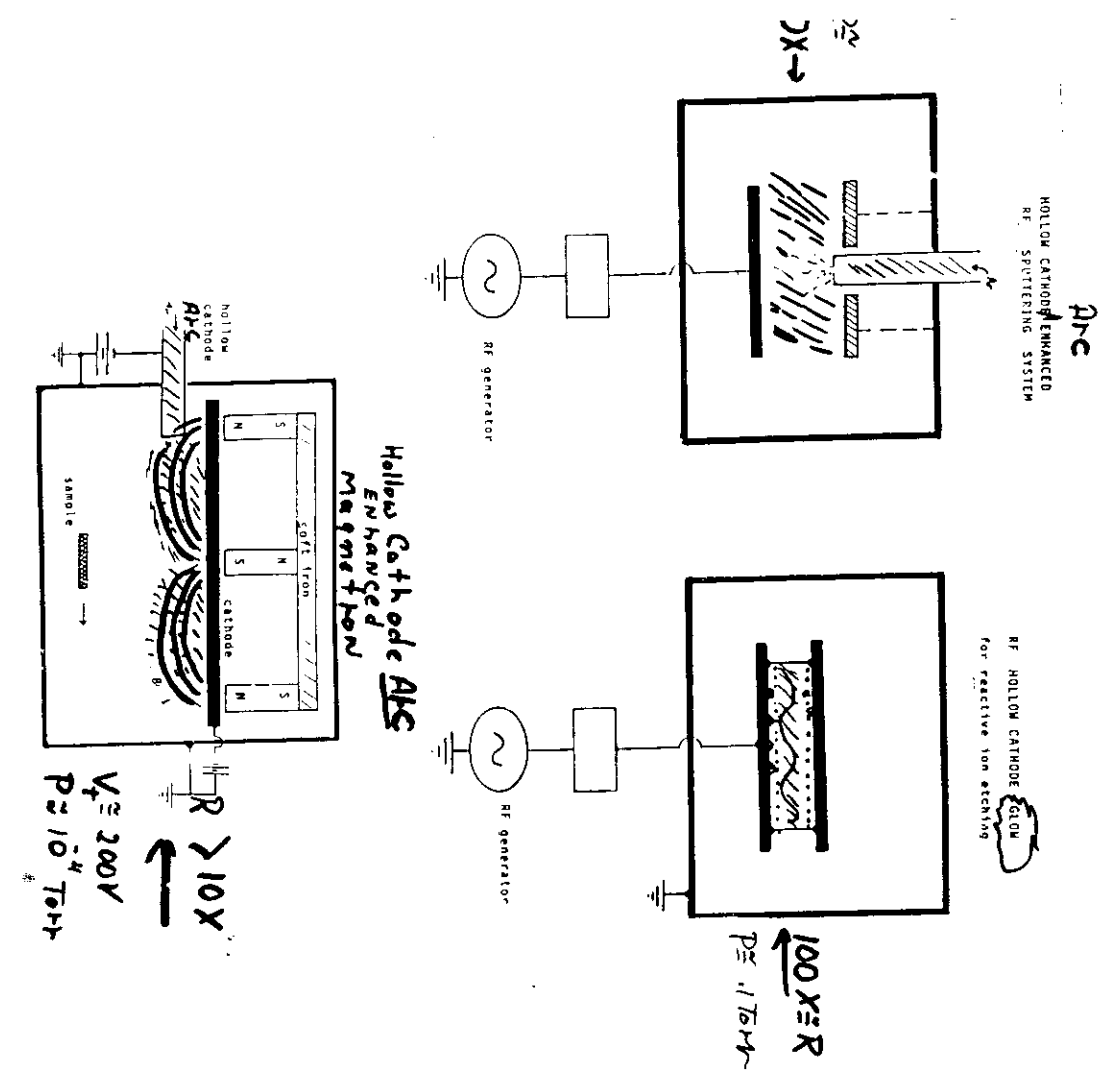

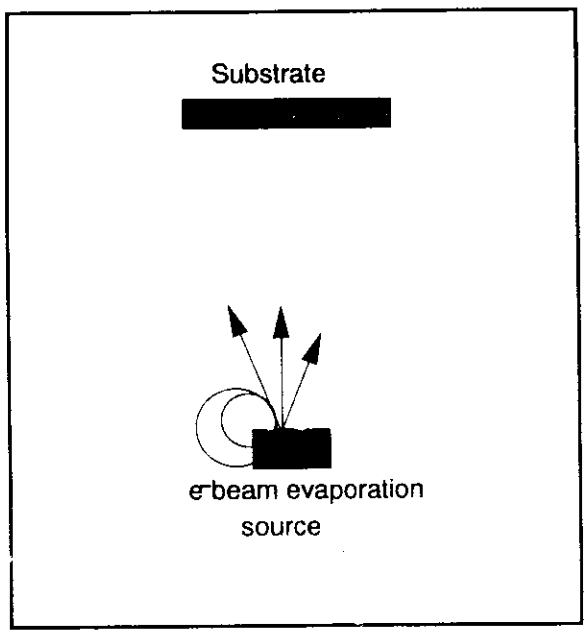

ELECTRON BEAM EVAPORATION

ION BEAM ASSISTED DEPOSITION

Directed Beam Deposition and Energetic Condensation

1. Collimated Sputtering

2. Cathodic Arc

3. Directed Ion Beam

Cross section of magnetron

By adding a collimator, the sputtered atom flux is effectively filtered: the atoms which do not pass the filter are collected on the inner surfaces of the collimator.

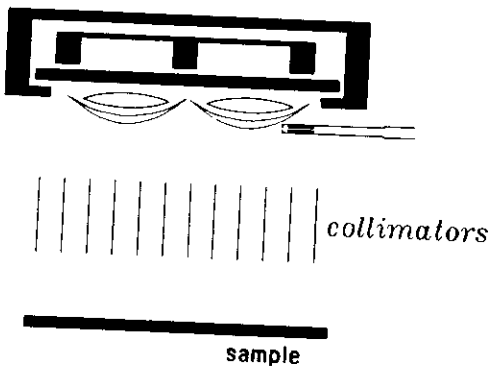

The collimator can be water cooled and grounded to protect sensitive samples

S.M. Rossnagel, IBM Research, PO 218 Yorktown Heights, NY 10598

DIAMOND THIN FILM MICROWAVE PROCESSING SYSTEM

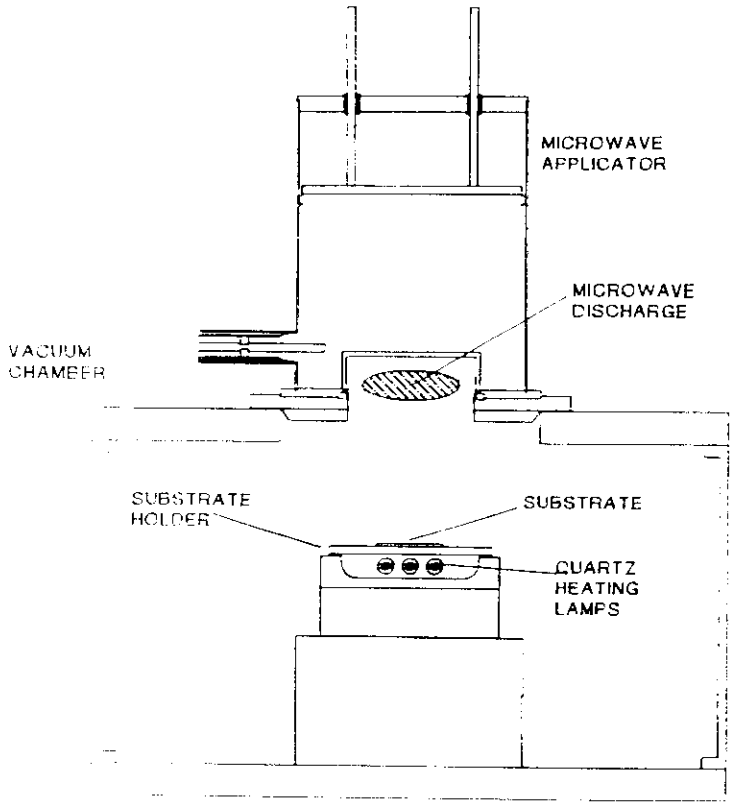

CENTRAL SCIENTIFIC SERVICES

ADVANCED MATERIALS LABORATORY

Laser, Ion Beam, Thermal & Plasma Carbon Films

J. J. Cuomo
J. P. Doyle
D. L. Pappas
K. L. Saenger
J. Bruley
R. Lossy
IBM Research Division
T. J. Watson Research Center
P. O. Box 218
Yorktown Heights, NY 10598-0218

IBM

Diamond-like Carbon
Amorphic Diamond
Energetic Condensation

Overview

Introduction

- Processes
  - Thermal
  - Plasma
  - Ion Beam
  - Laser
  - Other - Directed Ion Beam/Filtered Cathodic Arc
    - Considering
      - Average Energy
      - Energy Distribution of Particles

- Measurements
  - EELS
  - Resistivity
  - Optical
  - Density

- Temperature & Thermal Conducting Inverse Relationship with Density
- Model - Simple

Conclusion

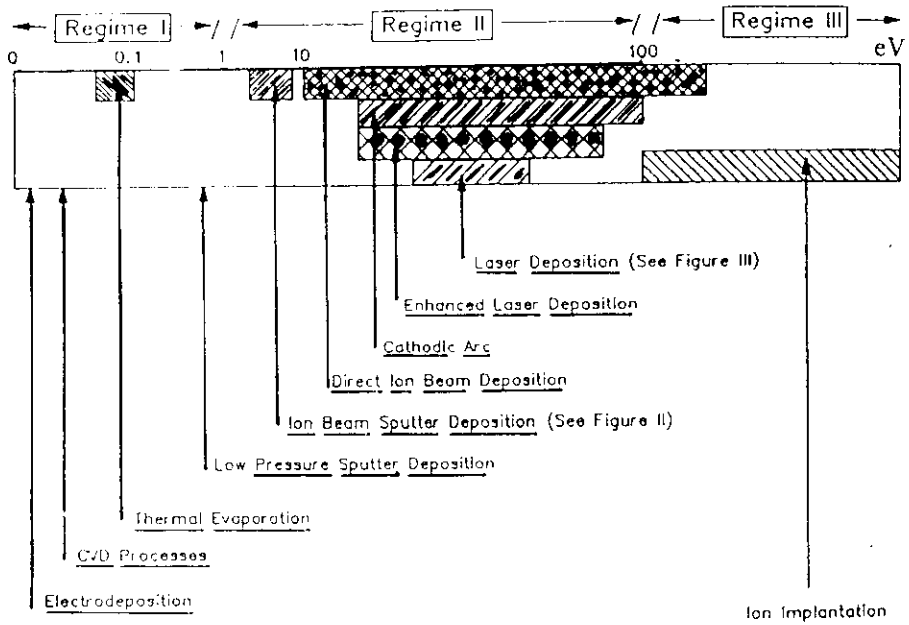

Figure 1: Diagram of the energy of the depositing species for several deposition process

"THE MATERIAL IS THE PROCESS"

JJC

Atoms, molecules, ions, electrons, and photons influence material properties

Deposition Technique	Energy Range (eV)
Thermal evaporation	0.05 - 1.
Diode sputtering	10. - 2000.
Magnetron sputtering	10. - 1000.
Ion beam sputtering	10. - 2000.
Ion plating	100. - 5000.
CVD	0.1 - 1.
LPE	0.1 - 1.

Processes

Process	Example	Average Partical Energy
Thermal	(e-beam)	~ 0.16eV
Plasma	Magnetron	~ 0.25eV - ~ 2.0eV
Ion Beam		~ 8.0eV
Laser	Excimer	~ 18.0eV
Other	Directed Ion Beam Filtered Calhodic Arc	~ 1→ 100eV

Regime I: Thermal

0.05 - 0.1 eV

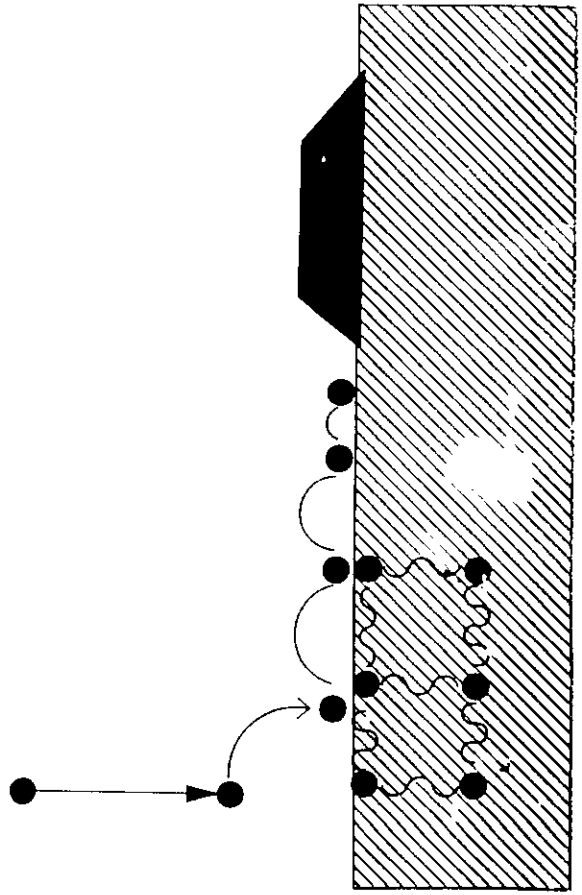

Region II: Thermal Quench (Attachment)

1.0 to 100 eV

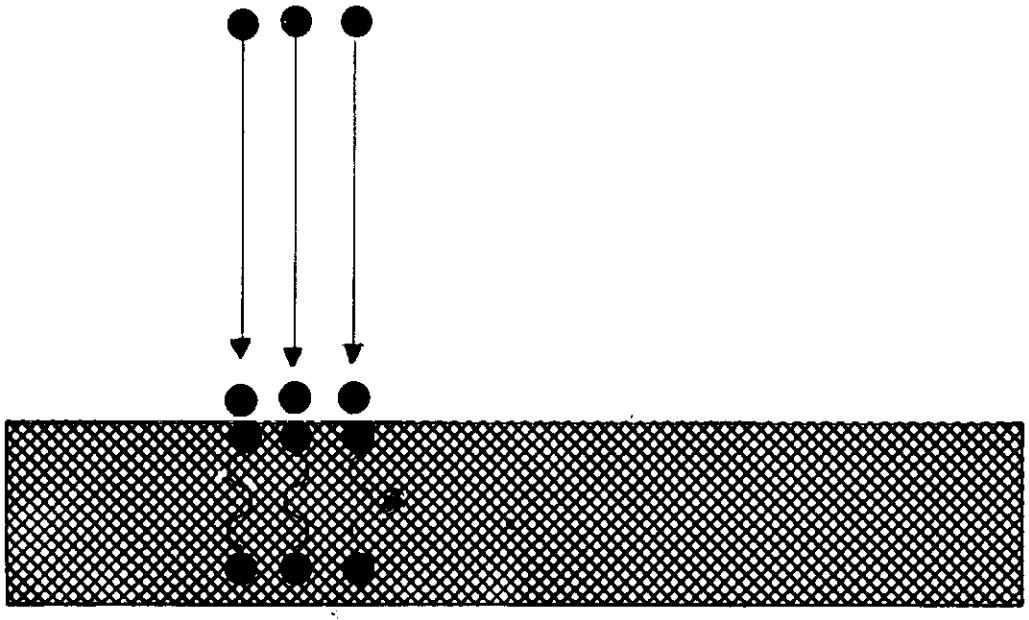

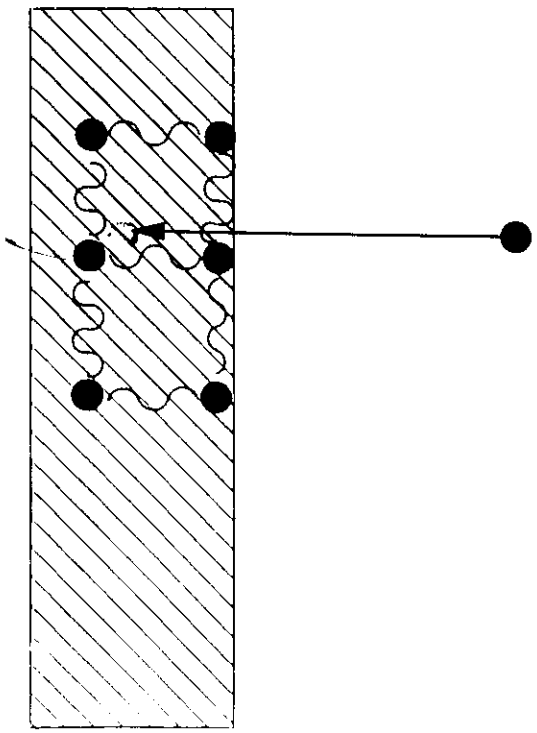

Regime III: Implantation

50 - 100 eV to KeV and Beyond

Substrate	Thermal Conductivity (W/cm*K) 77 K	300 K
Fused Quartz	0.0055	0.02
Quartz (⊥ to c)	0.3	0.06
Quartz (// to c)	0.6	0.1
Graphite (// to c)	0.68	0.8
Graphite (⊥ to c)	1.9	2.5
Tungsten	2.6	1.75
Copper	7.5	4
Silicon	13.4	1.4
Silicon (B-doped)	15	1.5
Silicon (P-doped)	15	1.5
Sapphire	15	0.2
Diamond type IIa	142	20

IBM

Table II. Thermal diffusivites (k) of substrates used in this study. Cu and graphite have been included for comparison.

SUBSTRATE	THERMAL DIFFUSIVITY ($cm^2\ sec^{-1}$) 300 K	77 K
type IIa diamond[a]	10.0	3300
Si[b]	0.880	30.0
NaCl[c]	0.330	0.267
sapphire[c] (60° to hex. axis)	0.147	46.6
Cu[b]	1.17	3.36
graphite[b] (pyrolytic, ‖ layer planes)	20.0	41.0
graphite[b] (pyrolytic, ⊥ layer planes)	0.095	0.57

[a]R. M. Chenko and H. M. Strong, General Electric Technical Information Series, Report No. 75CRD089, 1975.
[b]Y.S. Touloukian, *Thermophysical Properties of Matter* (IFI / Plenum, New York, 1973).
[c]calculated from $k = K / (C_p * \rho)$, where K is thermal conductivity, C_p is specific heat and ρ is density

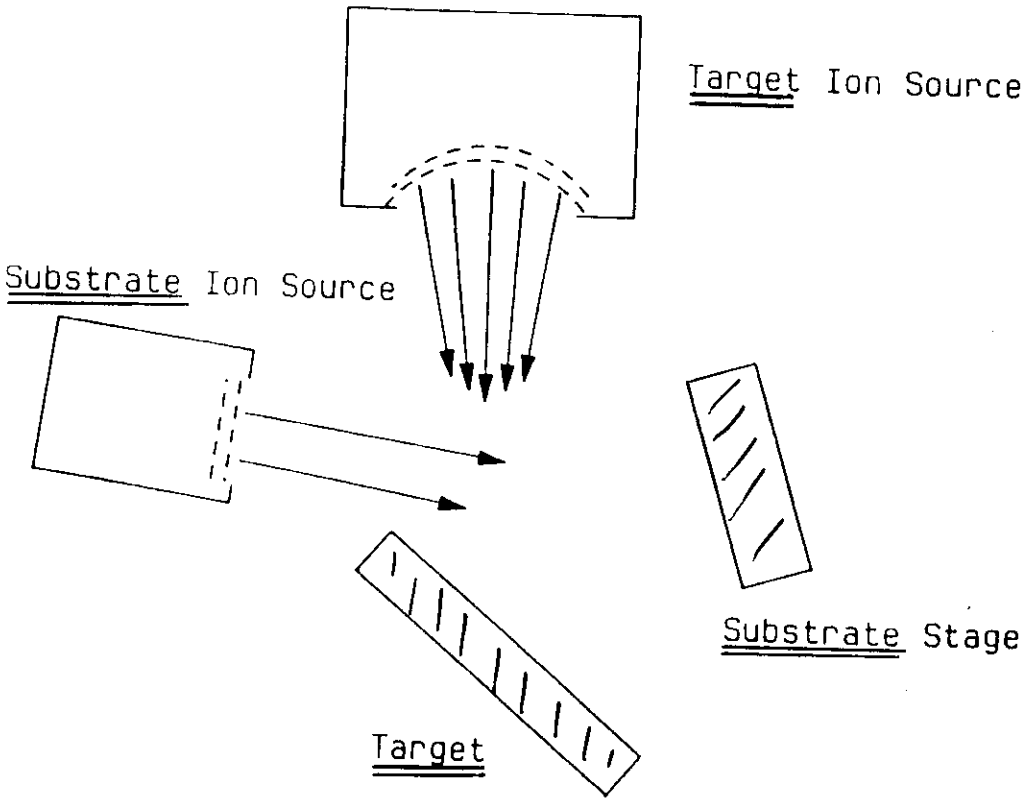

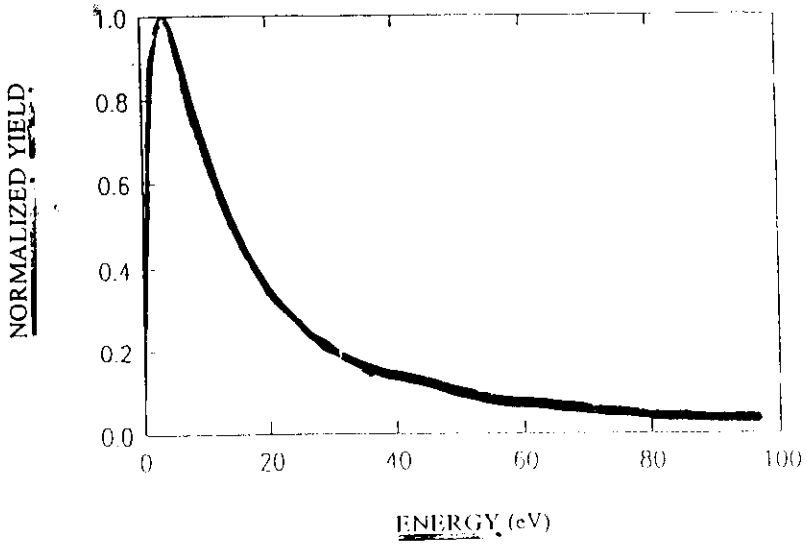

Figure 2: Energy distribution of carbon atoms sputtered from a carbon target.

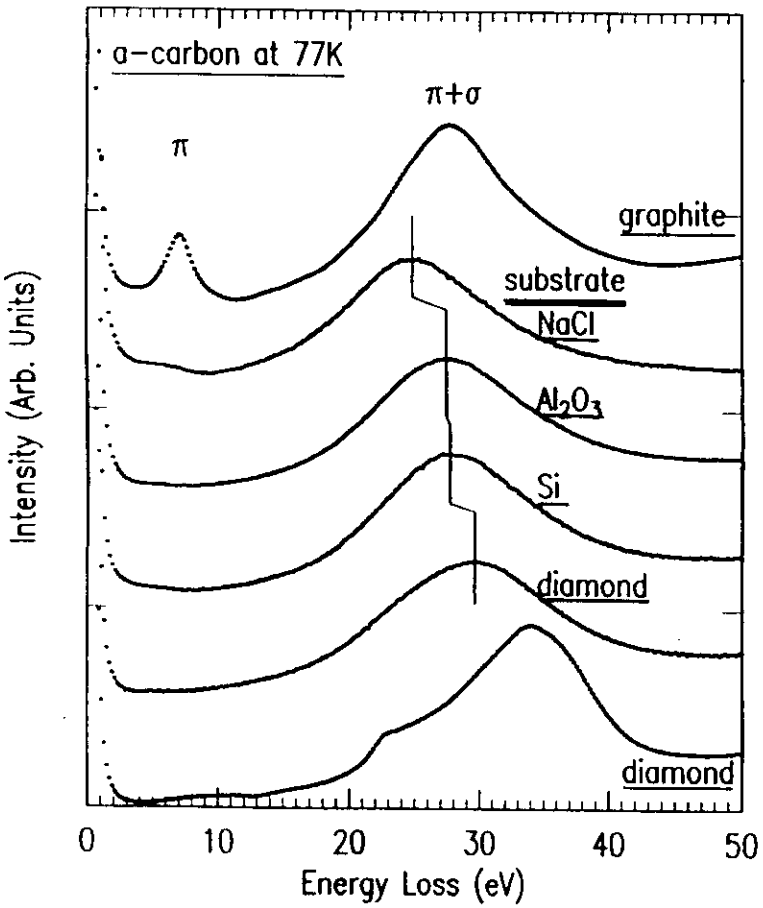

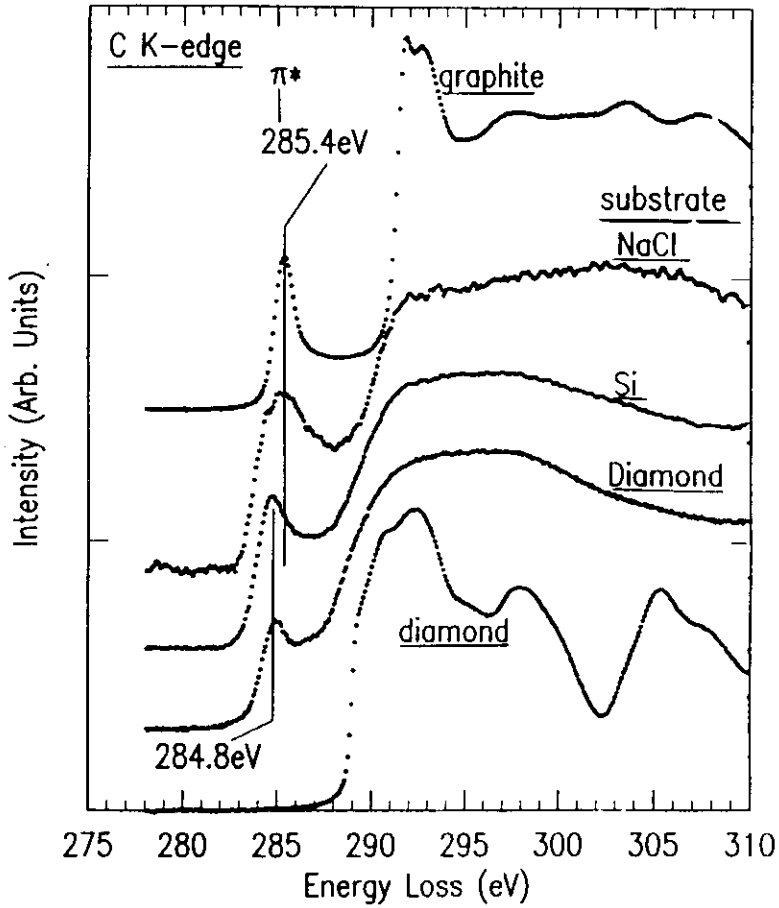

Amorphous Ion-Sputtered-Carbon onto 77K Substrate

Pulsed Laser Deposition

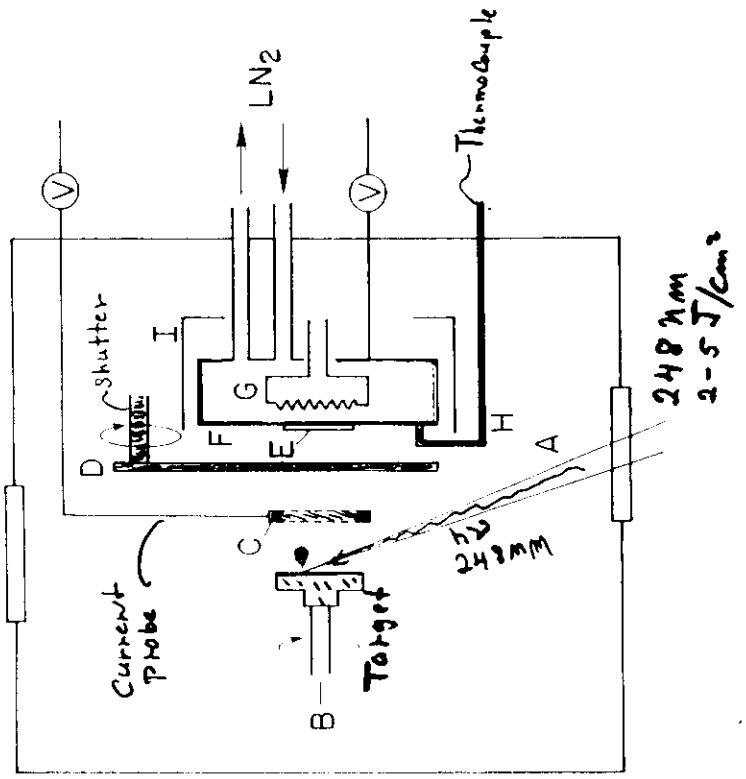

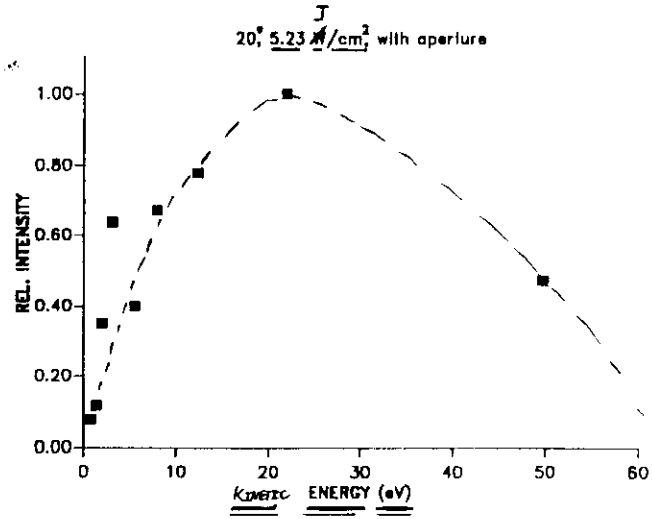

Fig 3.

Pappas 10/11/90

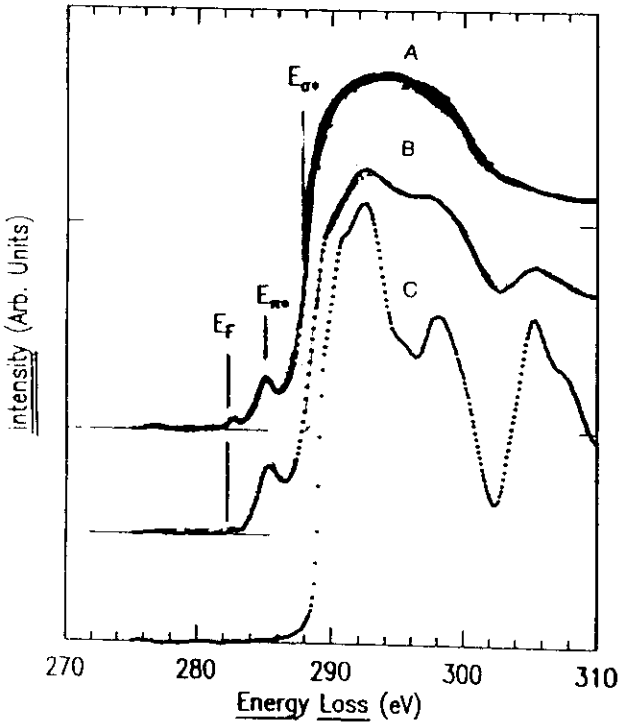

Figure 7: Electron energy loss data showing C(1s) K absorption edge for films deposited by laser deposition at 77 K. A) Type IIa diamond substrate. B) Type IIa diamond substrate. C) Natural diamond energy loss spectra.

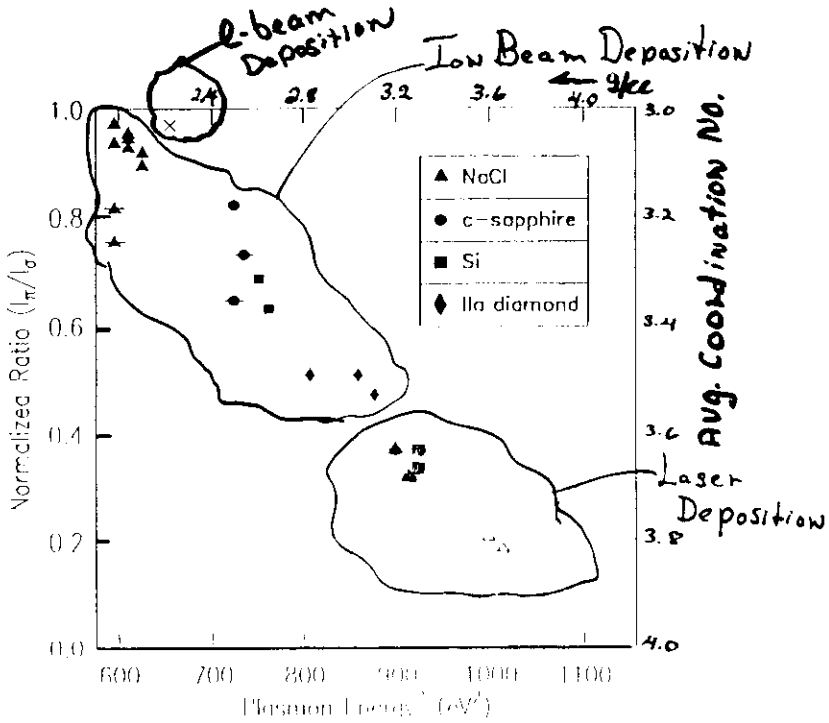

Figure 1. Summary of the EELS analysis for films deposited by a variety of methods at 295 K and 77 K. Plotted values are the relative normalized intensity of the π and σ contributions to the C K(1s) absorption edge vs. the square of the peak position of the bulk plasmon energy. The sp^3 number fraction, $\frac{sp^3}{sp^2+sp^3}$, denoted as $1-x$, is calculated from

$$1-x = \frac{3x}{4-x}$$

Apparent density (ρ) is determined using

$$\rho = \frac{1}{\frac{x}{\rho_g} + \frac{1-x}{\rho_d}}$$

in which ρ_g and ρ_d are the bulk densities of graphite (2.25 g/cm^3) and diamond (3.51 g/cm^3), respectively. The open symbols represent laser deposited films while the filled symbols indicate ion beam sputtered films. The X identifies an e-beam evaporated film. A dash ( ) through the symbol indicates depositions performed at 77 K.

Cathodic Arc

Fig 1

AKSENOV et. al.

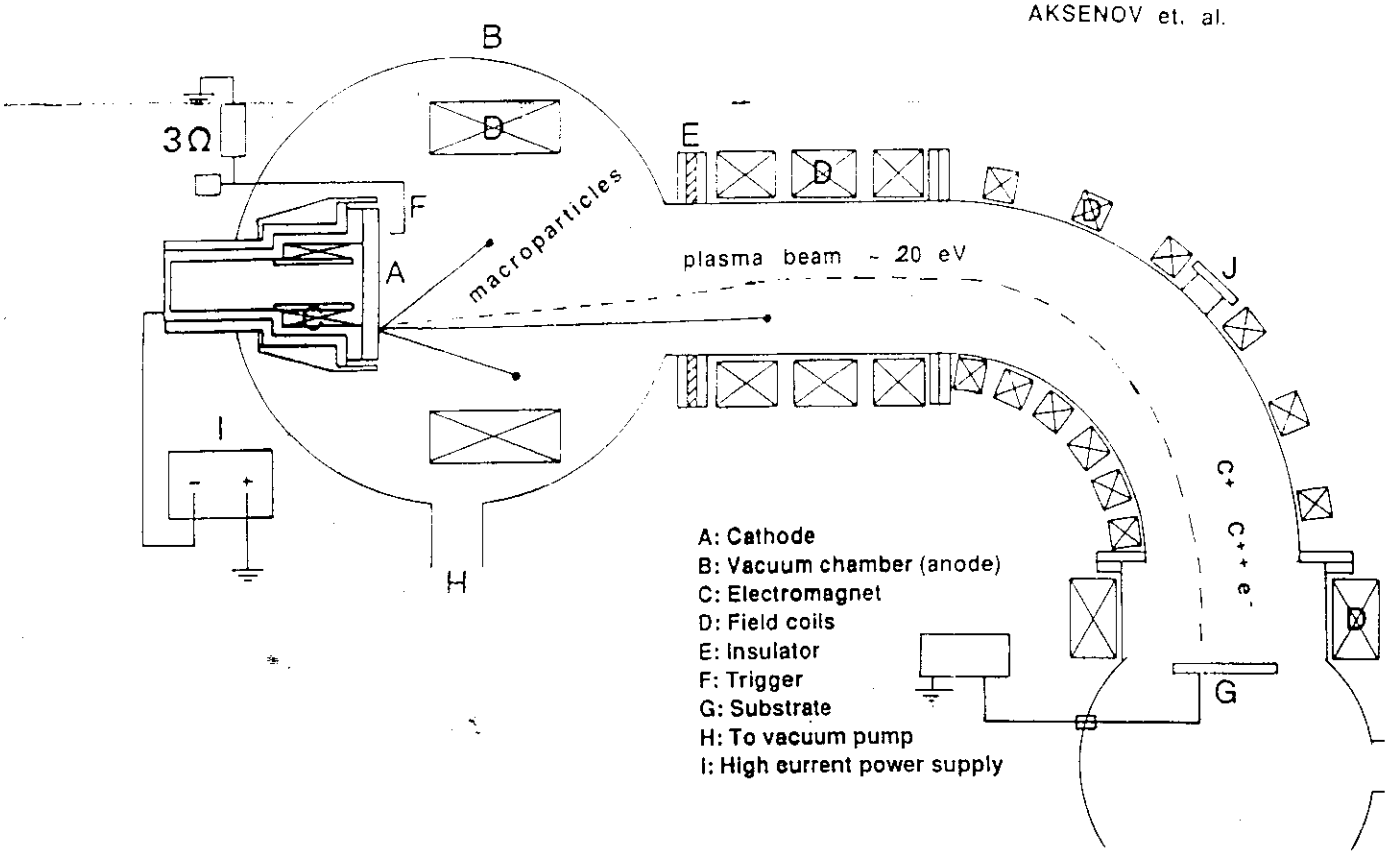

CATHODE SPOT PARAMETERS

		REFERENCE
CURRENT DENSITY	10^7 - 10^{10} Am^{-2}	DAALDER 1981
ELECTRON DENSITY	5 10^{20} m^3 (Cu)	BOXMAN 1974
ELECTRON TEMPERATURE (eV)	3-6 Cu 6 - 9 Al	BOXMAN 1974 BOXMAN 1974
PRESSURE	0.1 - 10 MPa	BERGMAN 1986
CRATER SIZE	1 - 20 μm	
CRATER FORMATION TIME	~ 10^{-7}s (JOULE) 1.2 - 4.5 ns Cu 1.6 - 6.2 ns Mo	DAALDER 1978 JÜTTNER 1981 (ION IMPACT)
ION ENERGY (eV)	25-75	DAVIS & MILLER 1979
ION FRACTION	0.1 - 1.0	PLYUTTO 1965

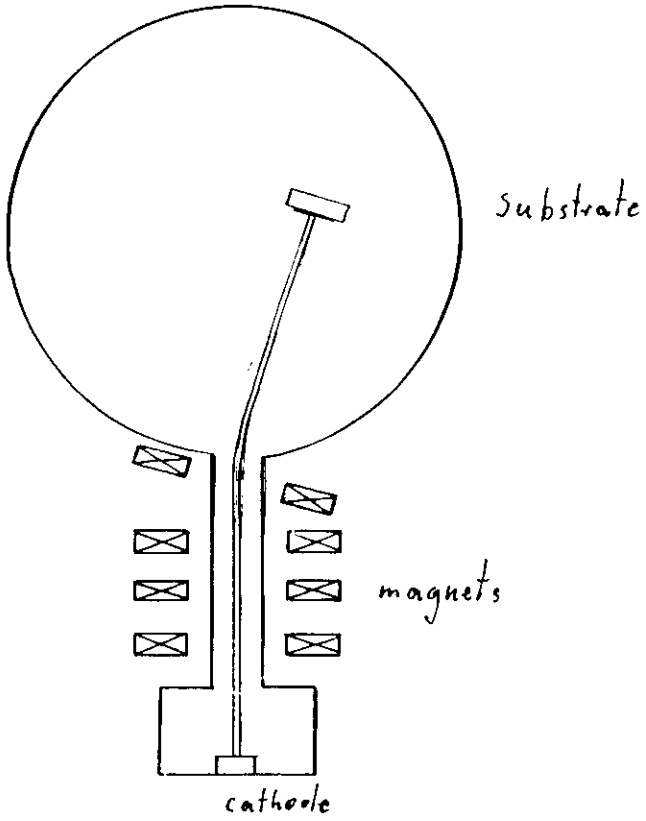
Substrate
magnets
cathode

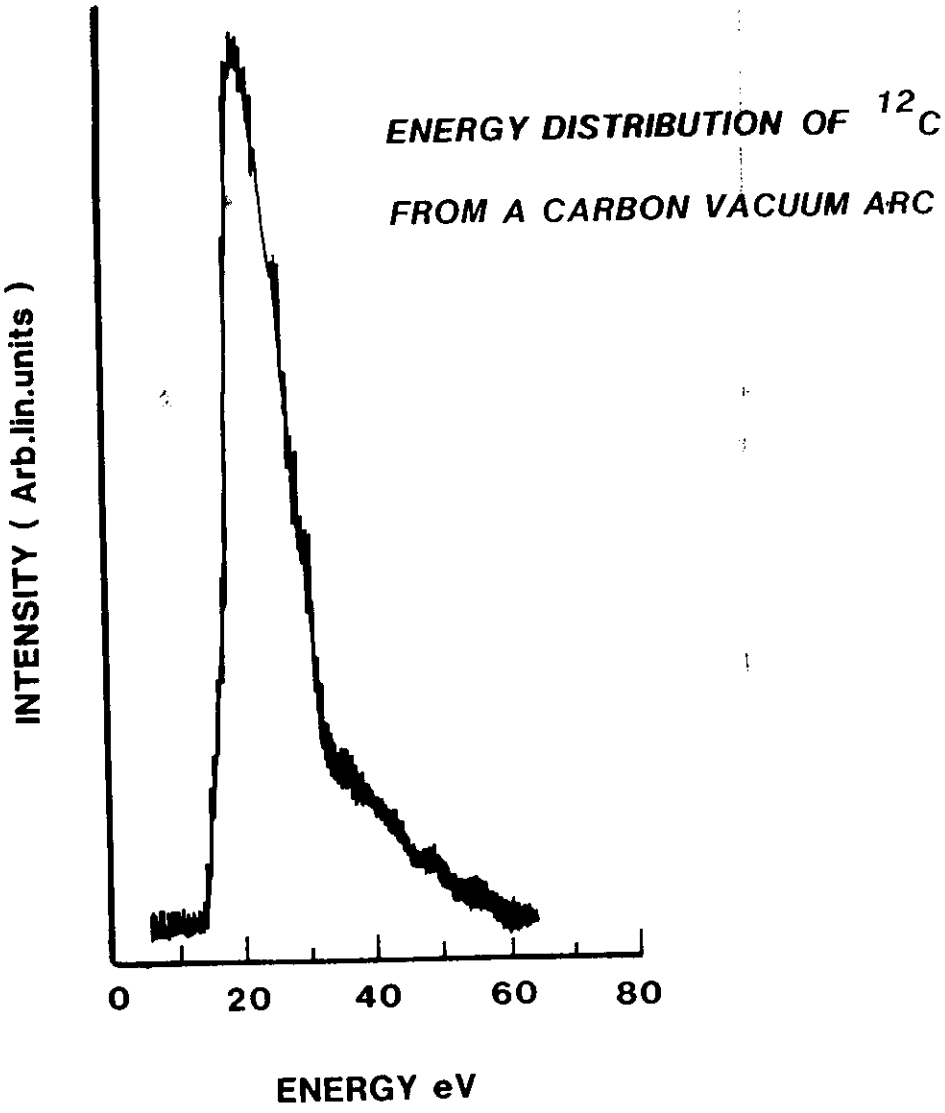
ENERGY DISTRIBUTION OF ^{12}C
FROM A CARBON VACUUM ARC
INTENSITY (Arb.lin.units)
0
20
40
60
80
ENERGY eV

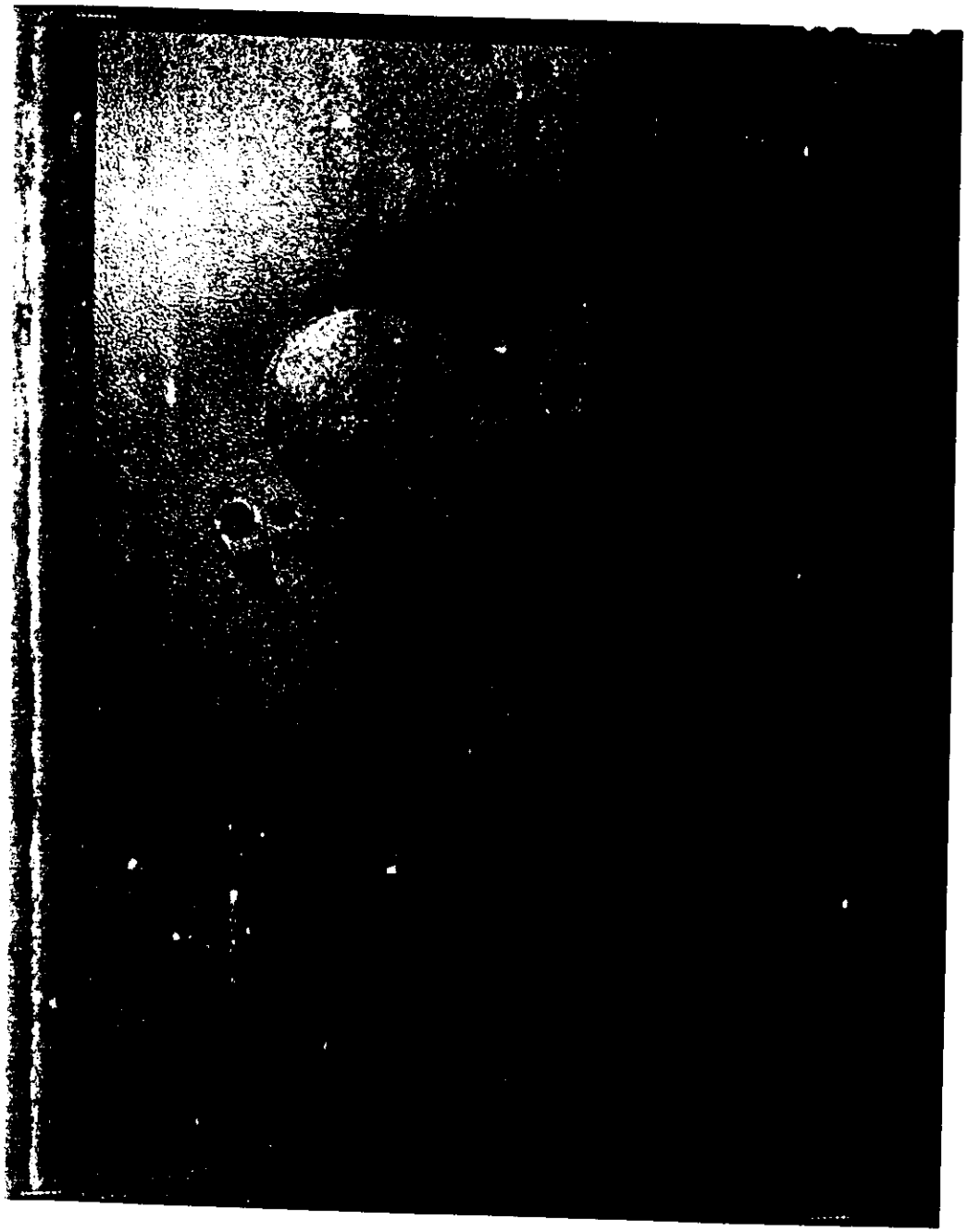

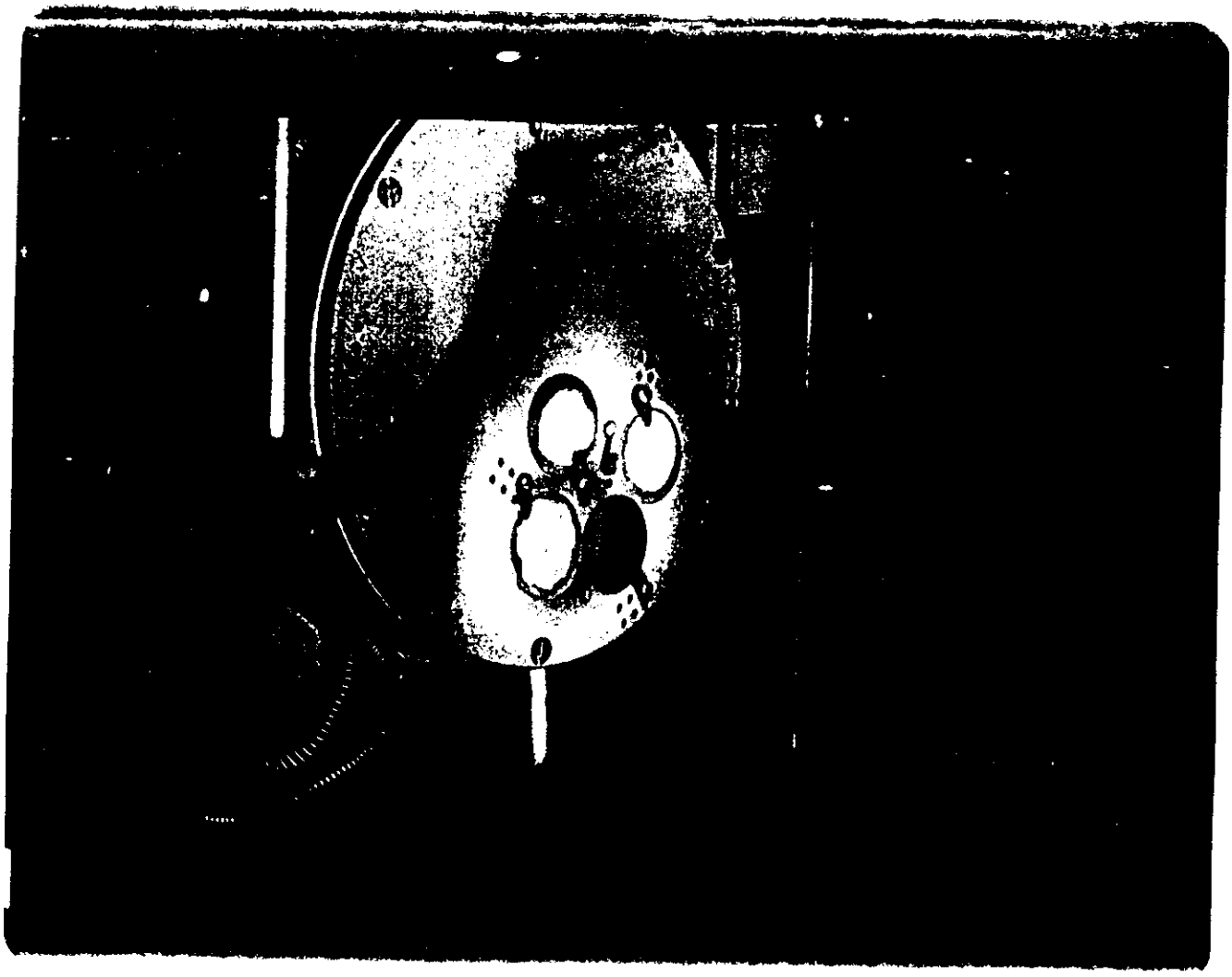

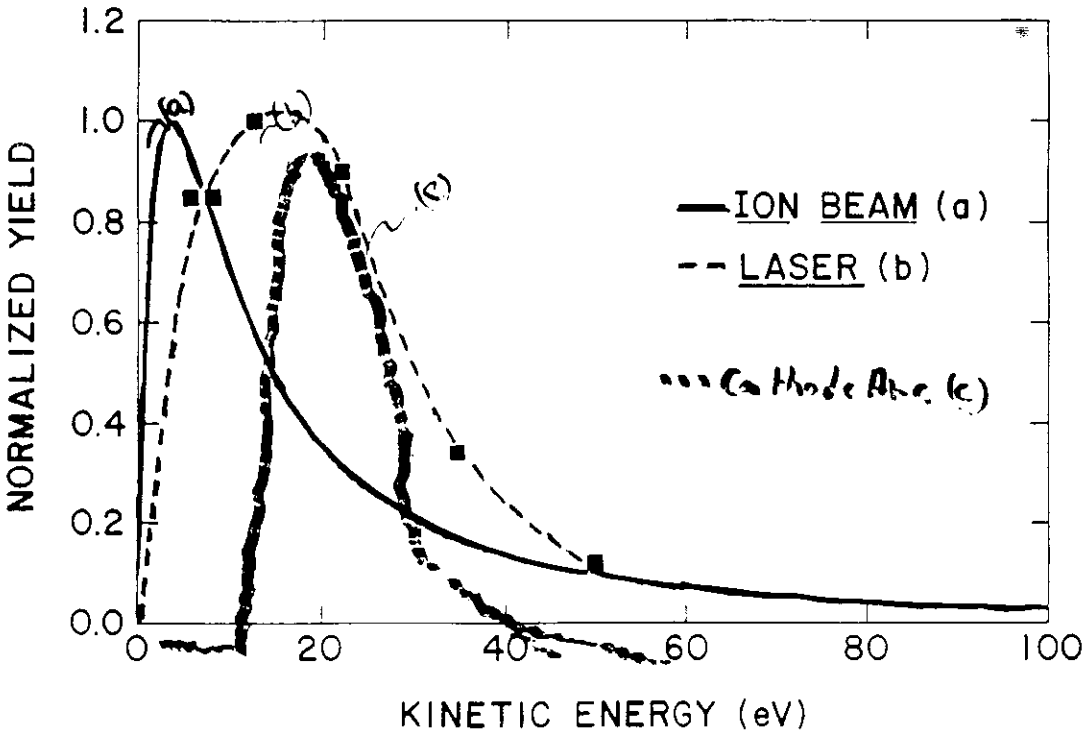
NORMALIZED YIELD
1.2
1.0
0.8
0.6
0.4
0.2
0.0
0
20
40
60
80
100
KINETIC ENERGY (eV)
(a)
(b)
(c)
ION BEAM (a)
LASER (b)
Cathode Arc (c)

Fig. 1

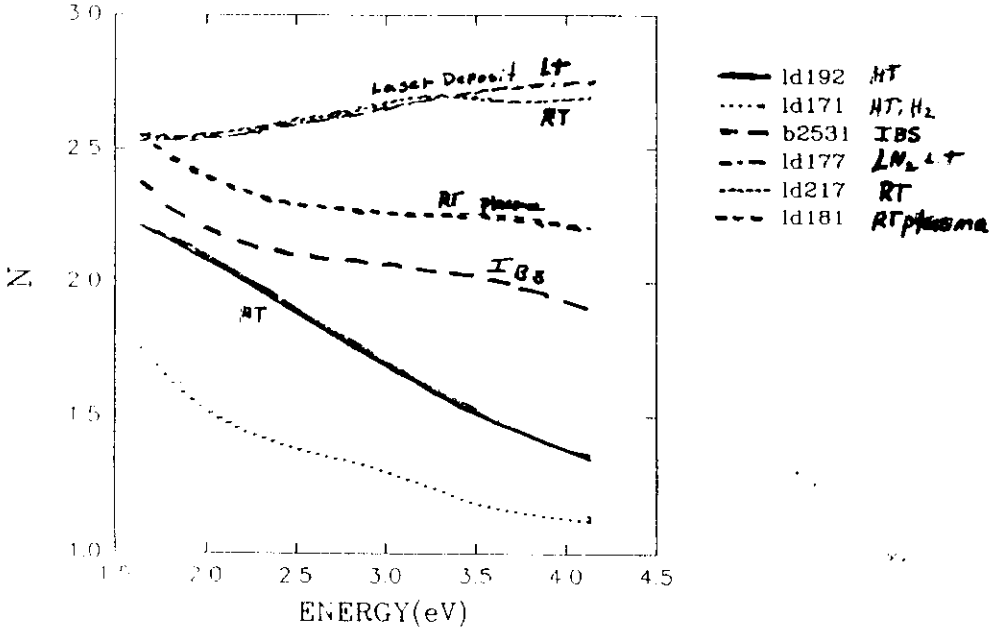

Fig. 2

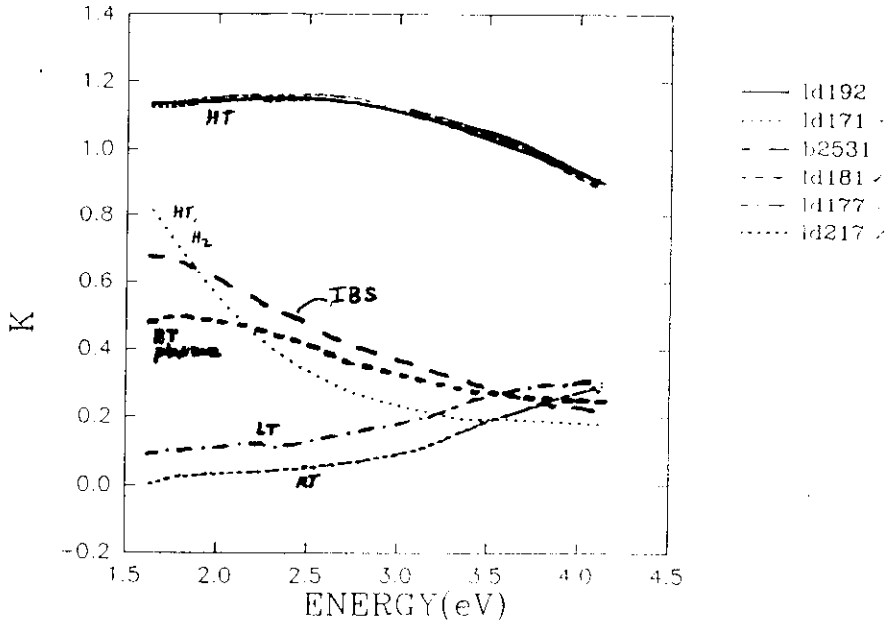

Index no. 2

	Process	SP^3/SP^2	Density gm/cc	N	K	Hardness GPa
Amorphous Carbon	Evaporation	0	~2.0	- -	- -	- -
Diamond-Like Carbon	PECVD	low?	~1.9-2.2	1.74	0.0065	15-30
Amorphous Diamond	Ion Beam	~50%	~2.9	2.05	0.29	- -
	Laser Beam	~75%	~3.3	2.55	0.042	90 (1100)
	Cathodic Arc	~85-90	>3.3	2.5	0.049	95 (1100)
Polycrystalline Diamond	PECVD	100%	3.5	2.41	~0	90-100 (1100)
Diamond	-----	100%	3.54	2.41	~0	90-1 (1100)

Temperature Stability			
	DLC	~350-400 °C	
	Amorphous Diamond	800 °C	in Vacuum
		850 °C	in Argon

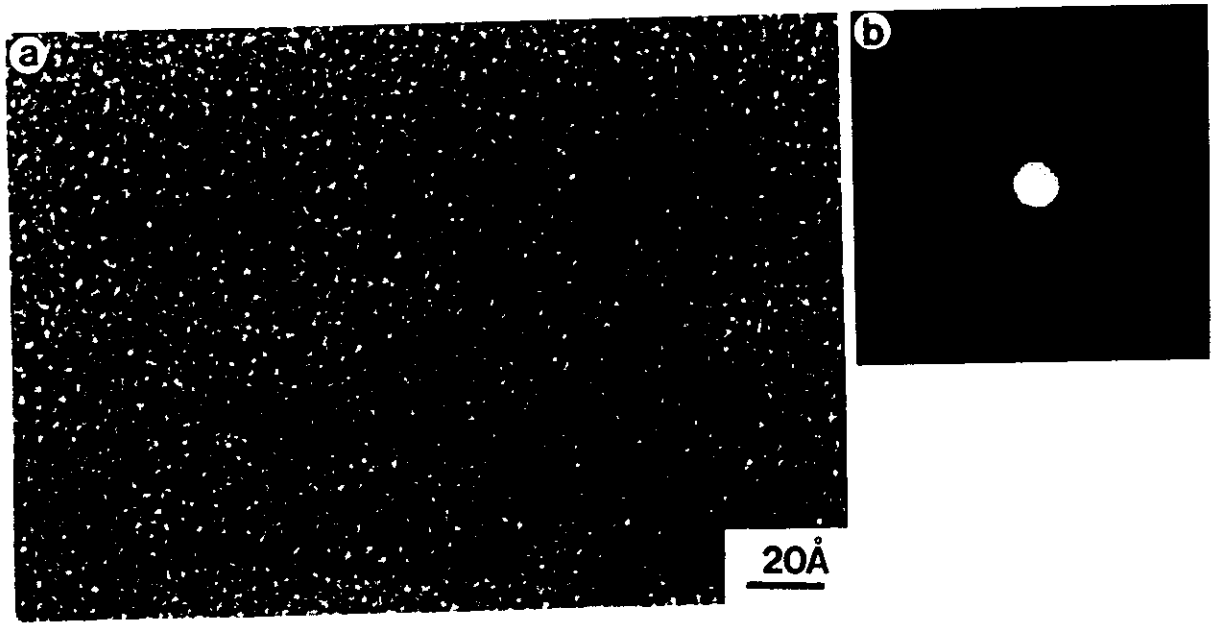

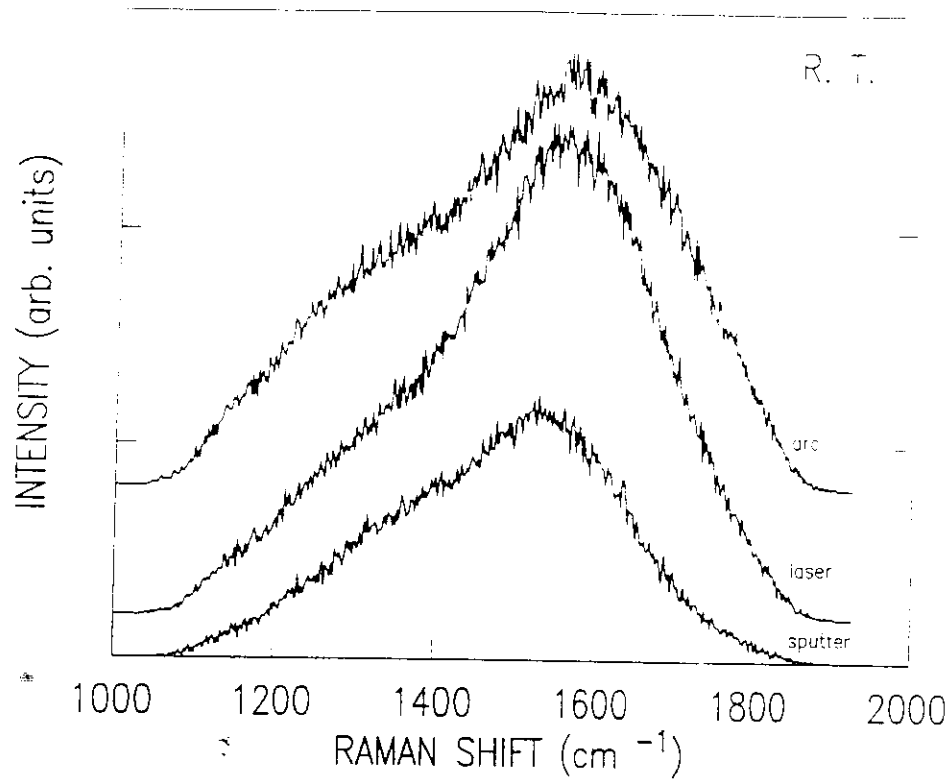
R. T.
INTENSITY (arb. units)
arc
laser
sputter
1000
1200
1400
1600
1800
2000
RAMAN SHIFT (cm $^{-1}$)

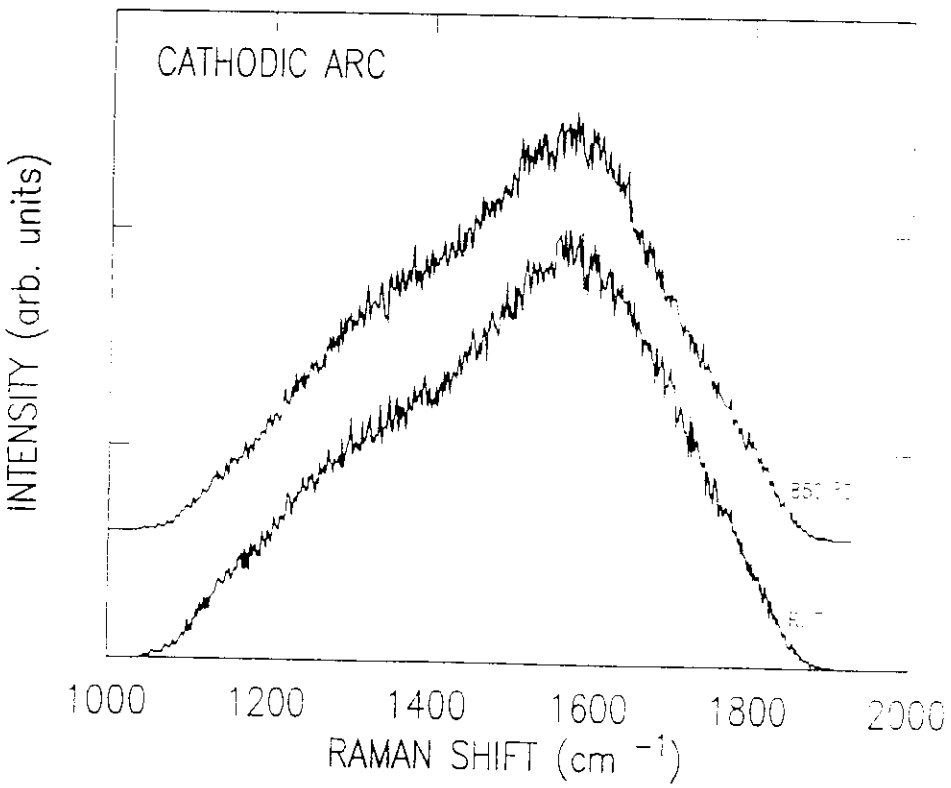
CATHODIC ARC
INTENSITY (arb. units)
1000
1200
1400
1600
1800
2000
RAMAN SHIFT (cm $^{-1}$)

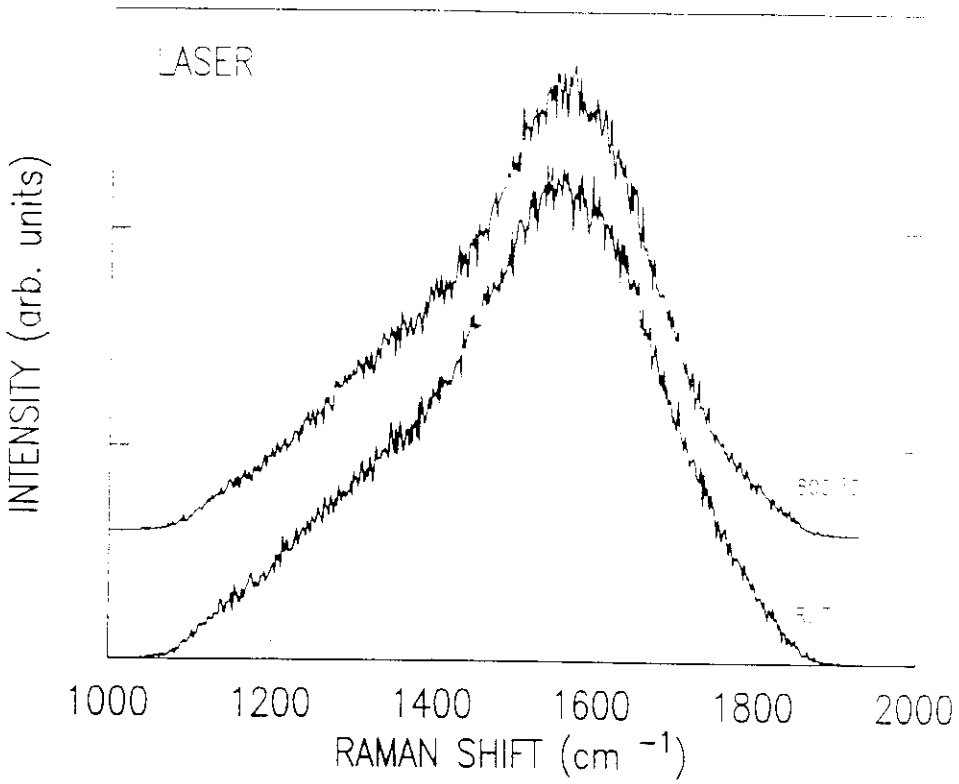
LASER
INTENSITY (arb. units)
1000
1200
1400
1600
1800
2000
RAMAN SHIFT (cm -1)

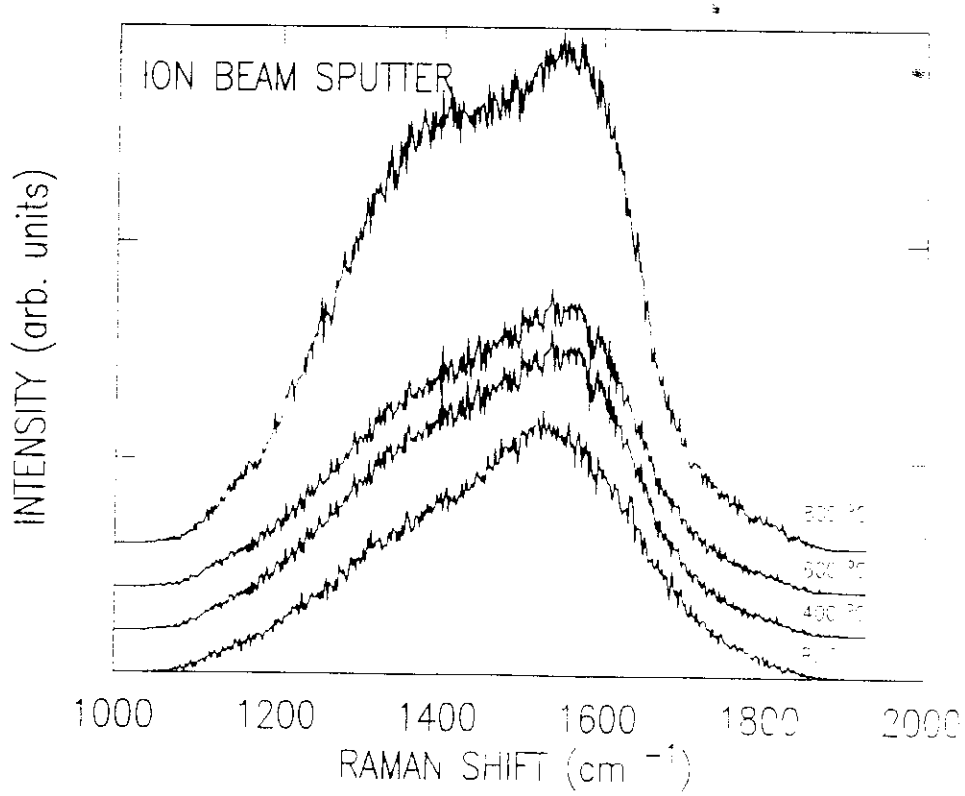
ION BEAM SPUTTER
INTENSITY (arb. units)
1000
1200
1400
1600
1800
2000
RAMAN SHIFT (cm -1)

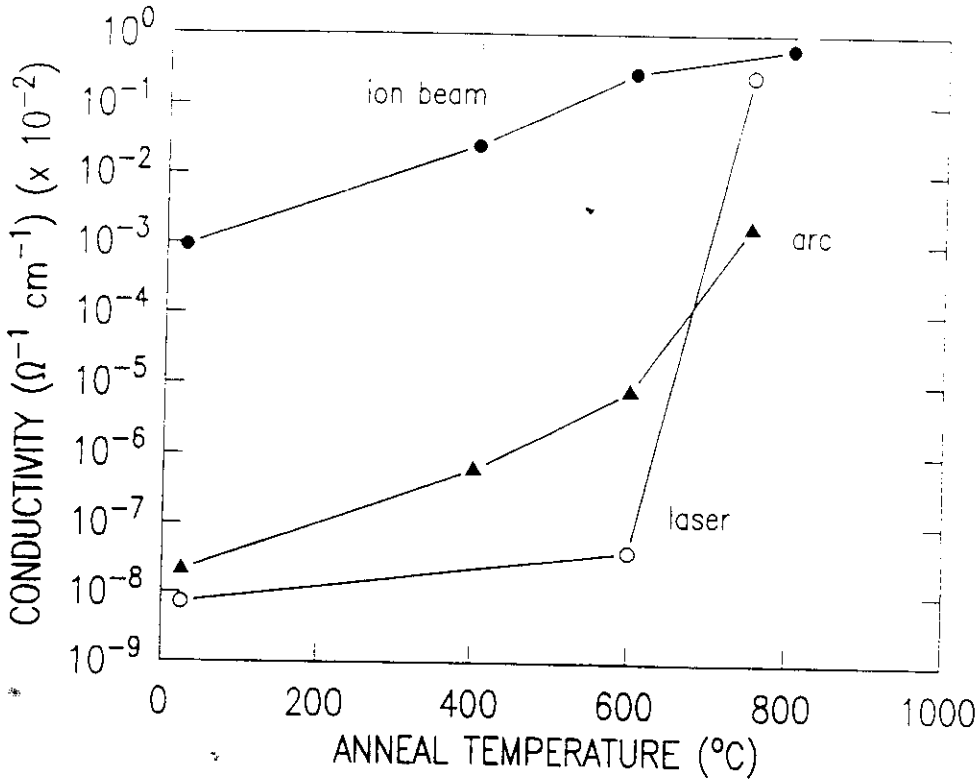

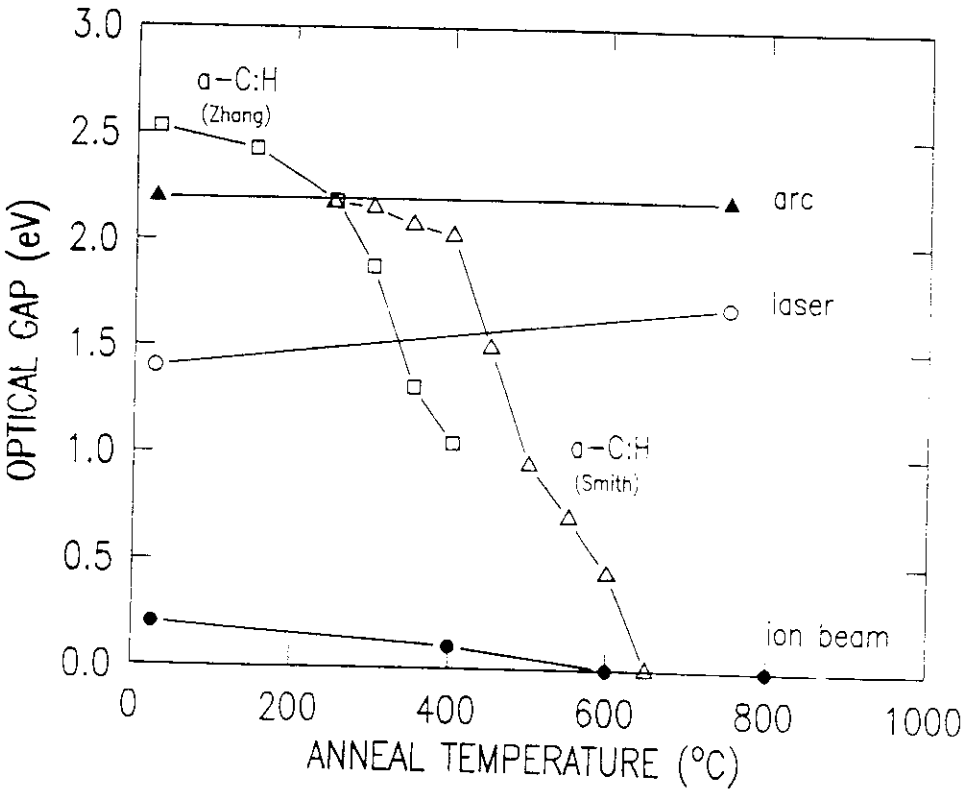

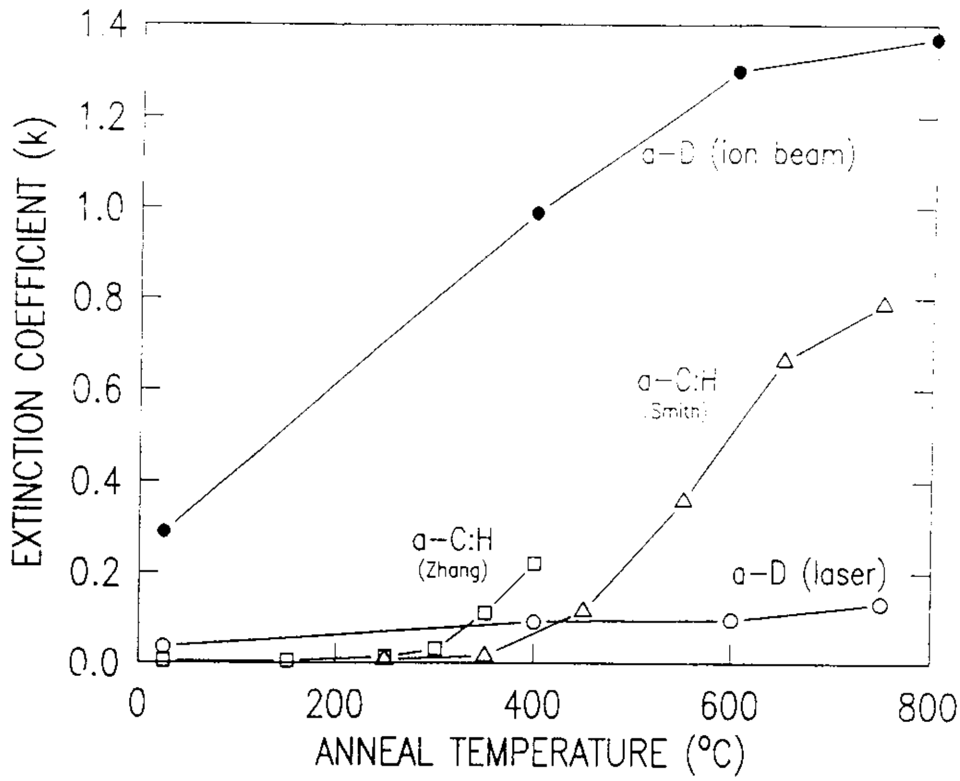

UGH3800 VOSSPLOT UGHBIN from PAPPAS at YKTVMV BEST 09/01/92 16 43.12 on THINFILM

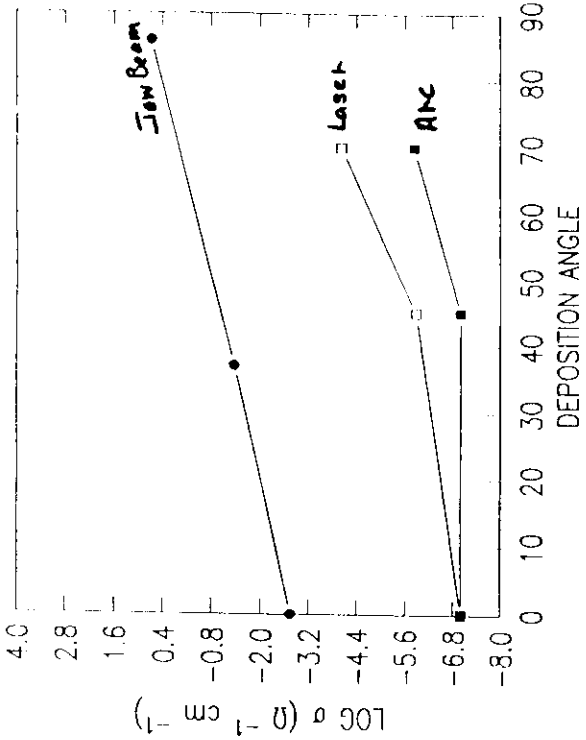

Relationship between conductivity and deposition angle for carbon films deposited onto fused quartz by cathodic arc (■——■), laser vaporization (□——□) and ion beam sputtering (●——●).

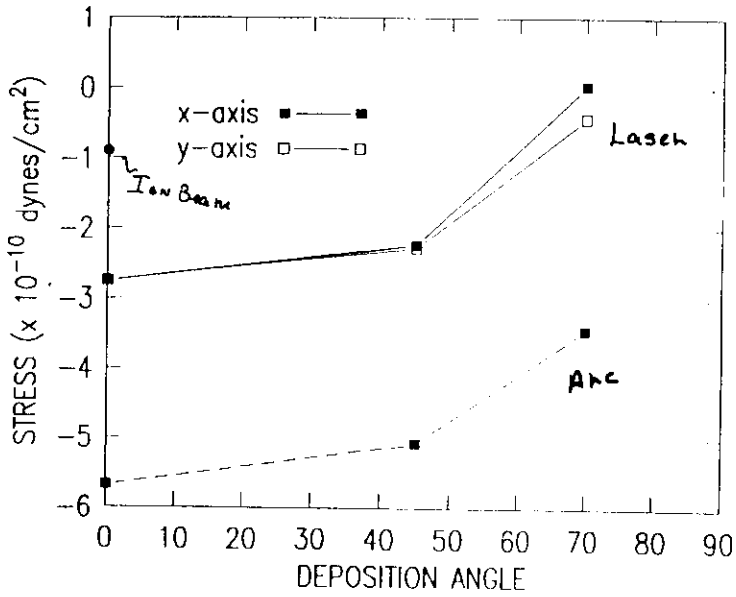

Relationship between film stress and deposition angle for carbon films deposited onto Si by laser vaporization (—) and cathodic arc (····) and ion beam sputtering (•, normal incidence only). Negative values denote compressive stress.

Filtered Cathodic Arc ~ 95% sp^3

Pulsed Laser ~ 86 % sp^3

Ion Beam ~ 50-60% sp^3

Evaporated ~100% sp^2

Sapphire